JOURNAL OF MATERIALS SCIENCE 11 (1976) 1135–1158

Review
Sialons and related nitrogen ceramics

K.H. JACK
The Wolfson Research Group for High-Strength Materials, The University of Newcastle upon Tyne, UK

Although silicon nitride is at present a leading contender for gas turbines and other high-temperature engineering applications, it is only the first of a wide field of nitrogen ceramics, other members of which offer better prospects for technological exploitation. "Sialons" are phases in the Si–Al–O–N and related systems and are comparable in variety and diversity with the mineral silicates. They are built up of one-, two-, and three-dimensional arrangements of $(Si, Al)(O, N)_4$ tetrahedra in the same way that the fundamental structural unit in the silicates is the SiO_4 tetrahedron. These new oxynitrides include structure types based upon α and β silicon nitrides, silicon oxynitride, aluminium nitride and silicon carbide, eucryptite, spinel, melilite and apatite. They are being explored for their thermal, mechanical, chemical and electrical properties.

1. Introduction

1.1. Engineering ceramics

The useable strength of a material is the stress that can be tolerated at a low strain, usually less than 0.1%, and so the requirement in a strong engineering ceramic is a high stress per unit strain, that is, a high elastic modulus. Even more desirable is a high value of the modulus divided by the specific gravity, that is a high usable strength to weight ratio (see Table I).

For a high elastic modulus the bond strength between atoms must be high and this implies covalent bonding. For a low density the atoms must have low atomic weights and small coordination numbers, and a small co-ordination number again implies covalent bonding. The high modulus materials also have high melting or high decomposition temperatures because this also depends on a high interatomic bond strength. Of the materials listed in Table I, aluminium nitride is easily hydrolysed, alumina has poor thermal shock resistance, beryllia has toxicity hazards, and carbon is readily oxidized. This leaves silicon nitride and silicon carbide as leading contenders for high-temperature engineering applications. It is also worth pointing out that, with the exception of beryllia, the examples given of high specific modulus materials involve atoms from the group silicon, aluminium, oxygen, nitrogen and carbon.

TABLE I Some high specific modulus materials

	Elastic modulus/ specific gravity 10^6 lb in.$^{-2}$	Melting or decomposition temperature (°C)
AlN	15	2,450
Al_2O_3	13	2,050
BeO	18	2,530
C whiskers	61	3,500
SiC	25	2,600
Si_3N_4	17	1,900
Steel, glass, wood	4	

1.2. Silicon nitride

The properties usually described for silicon nitride – its high strength, wear-resistance, high decomposition temperature, oxidation resistance, excellent thermal shock properties, low coefficient of friction and resistance to corrosive environments – should all make it the ideal engineering ceramic. However, one major difficulty is in fabricating shapes with these desirable properties. Because it is a covalently-bonded solid, the self-diffusivity of pure silicon nitride is very small and so it cannot be sintered to maximum density by firing.

© 1976 Chapman and Hall Ltd. Printed in Great Britain.

Two methods of shaping are used, giving what are called "reaction-bonded" and "hot-pressed" products.

In reaction bonding, the required shape is first made from compacted silicon powder which is then nitrided in molecular nitrogen at about 1400°C to give a product of mixed α- and β-silicon nitrides with about 25% porosity. The original dimensions of the silicon compact remain virtually unchanged during nitriding and so quite complex shapes can be obtained. The other route is to nitride powdered silicon to give α-silicon nitride powder. With suitable additives, for example 1 to 2 wt% magnesium oxide, this can be hot-pressed at 1 to 2 ton in^{-2} in a graphite die at 1700 to 1800°C to give a high-strength, maximum density, β-silicon nitride product.

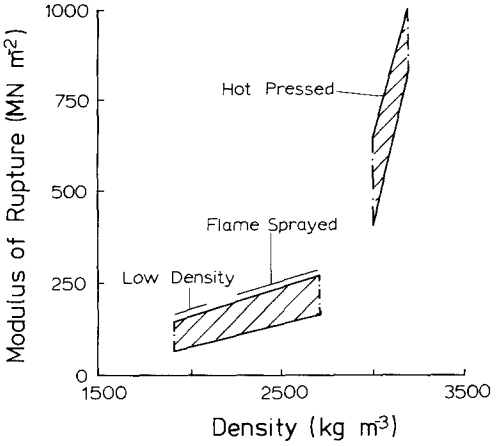

Figure 1 Relationship between strength and density for all forms of silicon nitride.

Fig. 1 illustrates a basic problem of silicon nitride technology. The highest strength material can be obtained only by hot-pressing and so it is limited to fairly simple shapes and is costly. On the other hand, reaction-bonded material can be fabricated easily but is porous and not strong enough for many applications. Also, with its higher surface area it is less oxidation resistant.

Although the use of silicon nitride as a ceramic was initially a British development [1,2], interest in recent years has been stimulated throughout the world by a 17 million dollar contract given to the Ford Motor Company and to the Westinghouse Electric Corporation by the Advanced Research Projects Agency of the American Department of Defence and aimed at demonstrating the use of brittle material in high-temperature engineering applications. It calls for two ceramic gas-turbine engines – a stationary one to produce 30 MW of electrical power, and the other suitable for a vehicle. Running at 1370°C compared with a present maximum of about 1050°C for nickel–chrome alloys these ceramic turbines will give improved efficiency, a better power:weight ratio, decreased costs, a saving in fuel and less atmospheric pollution. It has been suggested [3] that ceramic engines will be in limited production by 1982 followed by mass production in 1984 but the economic feasibility of this is still doubtful. All manufacturers want the properties of hot-pressed silicon nitride combined with the ease of fabrication of the reaction-bonded material. Even the hot-pressed product has its limitations as an engineering ceramic because the hot-pressing additive, usually magnesium oxide, reacts with the silica which is always present as a surface layer on the silicon nitride powder and gives either a glass or a second crystalline phase which impairs the high-temperature properties.

Distinct improvements have been made over the past two or three years in both hot-pressed and reaction-bonded silicon nitrides by reducing their impurities [4], but there is a limit to this approach. It has been argued [5] that even if absolutely pure starting material were economically feasible, hot-pressing either with or without an additive can never give a homogeneous, single-phase silicon nitride because of the surface silica on each powder particle. Where the second phase is vitreous it will soften at high temperatures, and second-phase inclusions, whether they are crystalline or vitreous, will act as stress raisers or will initiate cracks because of their differences in thermal expansion relative to the matrix.

It is suggested in the present paper that an alternative approach is to use the principles of ceramic "alloying" inherent in the production of "sialons", the name given [6] to phases in the silicon–aluminium–oxygen–nitrogen and related systems which were discovered independently in Japan [7,8] and England [9]. Silicon nitride is merely the first of a very wide field of nitrogen ceramics in which there seems to be excellent possibilities of designing materials starting from an atomic scale.

2. The sialons

2.1. The structures of nitrogen ceramics

Silicon nitride exists in two modifications, alpha and beta. As shown by Fig. 2, β is a typically

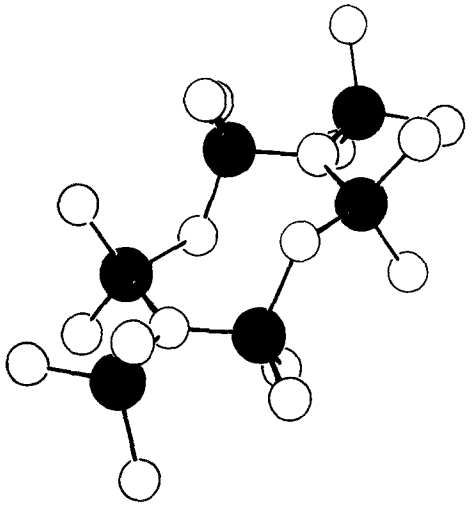

Figure 2 The crystal structure of β-silicon nitride.

covalent solid built up of SiN_4 tetrahedra joined in a three-dimensional network by sharing corners; each nitrogen corner is common to three tetrahedra. Alpha silicon nitride represents another way of joining together SiN_4 tetrahedra except that the present author, in spite of contrary views, believes that alpha prepared by nitriding silicon with molecular nitrogen has about one in every thirty nitrogen atoms replaced in its structure by oxygen [10].

In the Si–O–N system there is another phase, "silicon oxynitride" Si_2N_2O, which is potentially just as good a ceramic as silicon nitride [11]. It is built up of SiN_3O tetrahedra (see Fig. 3) and consists of parallel sheets of silicon–nitrogen atoms joined by Si–O–Si bonds.

The belief, whether or not it is correct, that α-silicon nitride is a defect structure in which a few nitrogen atoms are replaced by oxygen sugges-

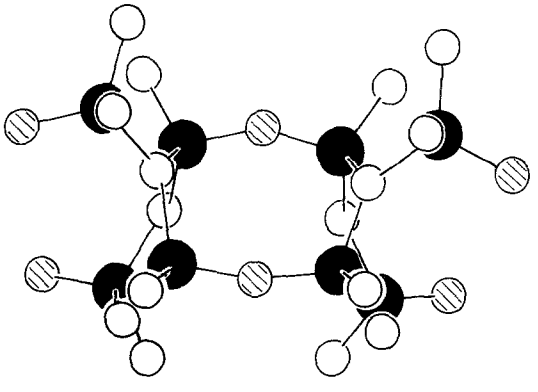

Figure 3 The crystal structure of silicon oxynitride, Si_2N_2O.

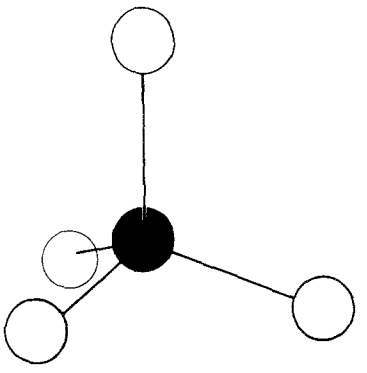

Figure 4 The tetrahedral unit in the silicates and in nitrogen ceramics.

ted that more nitrogen might be similarly replaced, without changing the structure, by applying the simple principles of silicate chemistry. In the mineral silicates, and in the various forms of silica itself, the building unit is the SiO_4 group carrying four negative charges; see Fig. 4. The tetrahedra may occur separately, or may be joined together by sharing oxygen corners into rings, chains, two-dimensional sheets, or three-dimensional networks. Aluminium plays a very special role in the silicate structures because the AlO_4 tetrahedron – this time with five negative charges – is about the same size as SiO_4 and can replace it in the rings, chains and networks provided that valency or charge compensation is made elsewhere in the structure. Thus, it seemed possible to replace N^{3-} by O^{2-} in silicon nitride if at the same time Si^{4+} was replaced by Al^{3+}. Charge compensation might also be feasible by introducing other metal atoms like Mg^{2+} and Li^{1+}. In fact, it was predicted [12] that a variety of new materials, vitreous as well as crystalline, could be obtained built up of silicon–aluminium–oxygen–nitrogen tetrahedra in the same way that the almost infinite range of silicates is built up of silicon–aluminium–oxygen units; see Table II. The structural unit of β-silicon nitride is SiN_4; of α it is on average $SiO_{0.1}N_{3.9}$; of silicon oxynitride it is $SiON_3$; and of the new "sialons" it is $(Si, Al)(O, N)_4$.

By coincidence, it seems that we discovered

TABLE II Structural units in some nitrogen ceramics

phase	structural unit
β-Si_3N_4	SiN_4
α-$Si_{11.5}N_{15}O_{0.5}$	$SiN_{3.9}O_{0.1}$
Si_2N_2O	SiN_3O
"Sialon"	$(Si, Al)(O, N)_4$

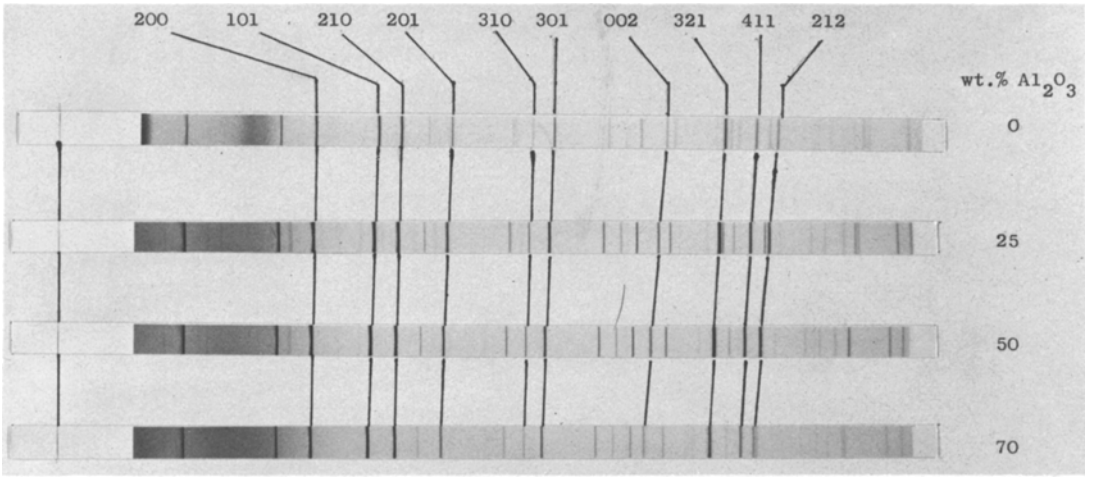

Figure 5 X-ray photographs of β'-sialons prepared by reaction of Si_3N_4 and Al_2O_3 at 2000° C.

these materials at about the same time as Oyama and his colleagues at Toyota [7] and Tsuge *et al.* at Toshiba [13]. The British and Japanese work has developed in similar directions and it is now apparent that we have even made the same mistakes.

2.2. Early experimental results

Fig. 5 shows X-ray photographs of the products [9] obtained by reacting together silicon nitride and alumina at 2000° C. The photographs are identical except that as the Al_2O_3 content increases up to about 70 wt% the X-ray reflections move to slightly lower angles. The structures are identical with that of β-Si_3N_4 and, therefore, the homogeneous sialon phase was termed β'. As Al^{3+} and O^{2-} replace Si^{4+} and N^{3-} the metal:non-metal atom bond-lengths increase and so the β' hexagonal unit-cell dimensions also increase. The following alternative compositions for β' were considered:

$$\begin{array}{ll} \beta & Si_6^{24}N_8^{\overline{24}} \\ \downarrow & \\ \beta' & Si_{6-0.75x}^{24-3x}Al_{0.67x}^{2x}O_x^{\overline{2x}}N_{8-x}^{\overline{24-3x}} \qquad (1) \\ \searrow & \\ & Al_{5.33}^{16}O_8^{\overline{16}} \equiv Al_2O_3 \end{array}$$

$$\begin{array}{ll} \beta & Si_6^{24}N_8^{\overline{24}} \\ \downarrow & \\ \beta' & Si_{6-z}^{24-4z}Al_z^{3z}O_z^{\overline{2z}}N_{8-z}^{\overline{24-3z}} \qquad (2) \\ \searrow & \\ & Al_6^{18}O_6^{\overline{12}}N_2^{\overline{6}} \equiv Al_2O_3 \cdot AlN. \end{array}$$

and on the basis of limited chemical analysis and the observations of only one single-phase crystalline product, it was concluded that sequence 1 represented the reaction between silicon nitride and alumina. It was not appreciated that products represented by sequence 2 might be obtained with (i) volatilization of silicon monoxide and nitrogen or, in the reducing environment of graphite in the hot press, (ii) volatilization of silicon and carbon monoxides, or (iii) with simultaneous formation of a silica-rich glass. For example, possible reactions to produce β' with $z = 4$ are:

$$4Si_3N_4 + 6Al_2O_3 = 3Si_2Al_4O_4N_4 + 6SiO + 2N_2 \quad (i)$$

$$Si_3N_4 + 2Al_2O_3 + C = Si_2Al_4O_4N_4 + SiO + CO \quad (ii)$$

$$Si_3N_4 + 2Al_2O_3 = Si_2Al_4O_4N_4 + SiO_2 \quad (iii)$$

Similar β'-sialon phases were obtained by reacting silicon nitride with lithium-aluminium spinel, $LiAl_5O_8$, and also with magnesium–aluminium spinel, $MgAl_2O_4$. The structures, identical with that of β-Si_3N_4 (see Fig. 6) contained lithium and magnesium respectively. The metal:non-metal atom-ratio $M/X = 3/4$ in the reacting spinels is, of course, the same as that in the silicon nitride. Subsequently, Si_3N_4 was reacted with equi-molecular mixtures of Al_2O_3 and AlN (that is, the equivalent of the spinel $Al_3O_3N \equiv Al_2O_3 \cdot AlN$) and then with varying ratios of the oxide and nitride. From the results it was concluded that the β'-phase field extended not only along the joins Si_3N_4–Al_2O_3 and Si_3N_4–Al_3O_3N but also covered the region between these limits. The phase diagram deduced for the Si_3N_4–Al_2O_3–AlN system at above 1700° C (Fig. 7a) was identical with that proposed by Oyama [14]

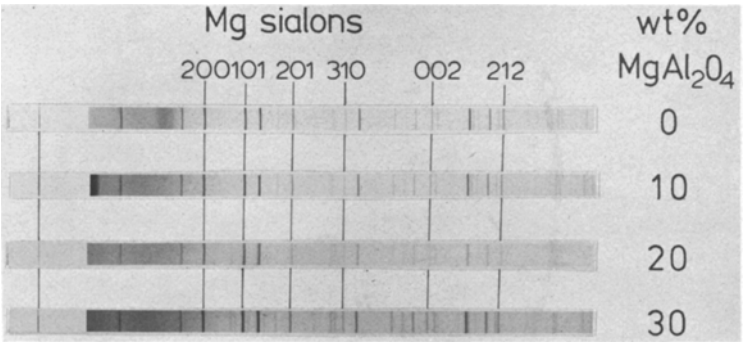

Figure 6 X-ray photographs of β'-magnesium sialons prepared by reaction of Si_3N_4 and $MgAl_2O_4$ at 1700° C.

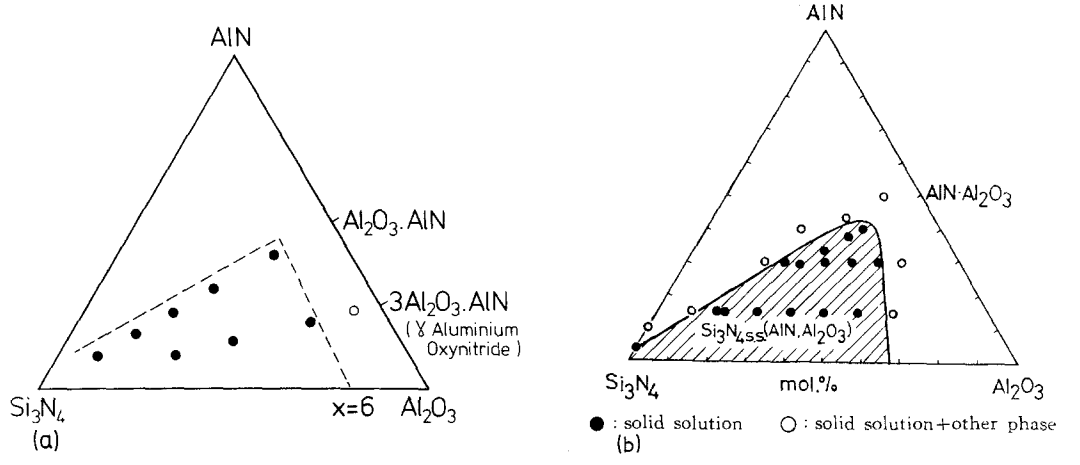

Figure 7 Phase diagrams for the Si_3N_4–Al_2O_3–AlN system above 1700° C. Both now known to be incorrect. (a) From results at Newcastle; (b) proposed by Oyama [14].

(see Fig. 7b), but both are now known to be incorrect.

Doubts about this range of homogeneity for β' were raised by Lumby, *et al.* [15] who suggested from creep measurements that sialons with overall compositions along the Si_3N_4–Al_2O_3 join contained glassy phases whereas compositions with M/X = 3/4 showed minimum high-temperature creep. Since then, preparative work at Stuttgart [16] and Newcastle [17] using mixtures of different reactants (e.g. from Si_3N_4, Al_2O_3, AlN, Si_2N_2O, SiO_2) to obtain the same product has shown that β' extends along the join Si_3N_4–Al_3O_3N from $z = 0$ to about $z = 4.2$. The range of homogeneity with M/X unequal to 3/4 is quite limited.

In addition to the sialon phases α', β', O′ and X originally reported [6, 9], Gauckler *et al.* [16] prepared six unidentified phases nearer to the AlN corner of the Si_3N_4–AlN–Al_2O_3–SiO_2 system and with ranges of homogeneity extending along lines of constant M/X ratio. These have now been identified at Newcastle [18] as defect tetrahedral polytypes of AlN. Before considering these, it is necessary to discuss the representation of sialon systems.

3. The representation of the Si–Al–O–N and related systems

The Si–Al–O–N system is apparently four-component and so might be represented by a regular tetrahedron (see Fig. 8) each of the vertices of which represent one atom of the respective elements. An point within the tetrahedron is the equivalent of one atom of composition

$$Si_aAl_bO_cN_{1-(a+b+c)}$$

but if in any phase the combining elements have their accepted valencies Si^{IV}, Al^{III}, O^{II} and N^{III}, one degree of freedom is lost and it is easily shown that the composition is given by

$$Si_aAl_bO_{3-7a-6b}N_{6a+5b-2}.$$

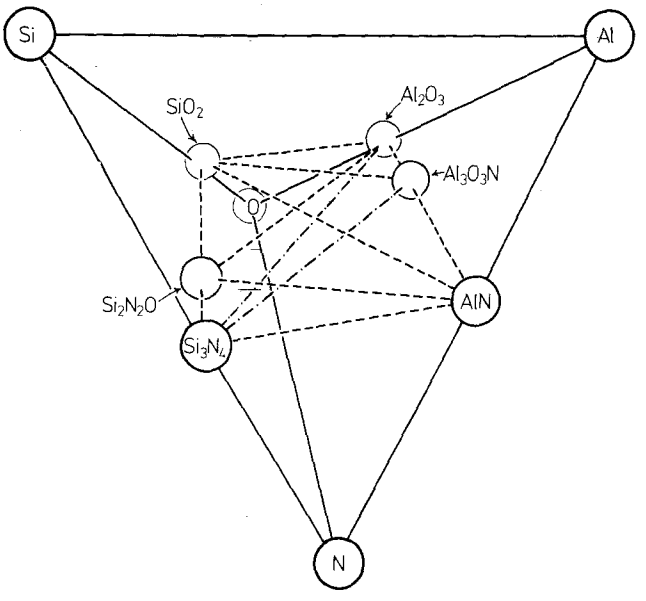

Figure 8 The tetrahedral representation of the Si–Al–O–N system.

The system is then a pseudo-ternary one. If the tetrahedron of Fig. 8 is described in terms of three orthogonal axes x, y and z with corners:

oxygen at co-ordinates	0, 0, 0
silicon at	1, 0, 1
aluminium at	0, 1, 1
and nitrogen at	1, 1, 0

the compositions of all solid phases then lie on the irregular quadrilateral plane $(0\,1\,\bar{6})$ shown in Fig. 9

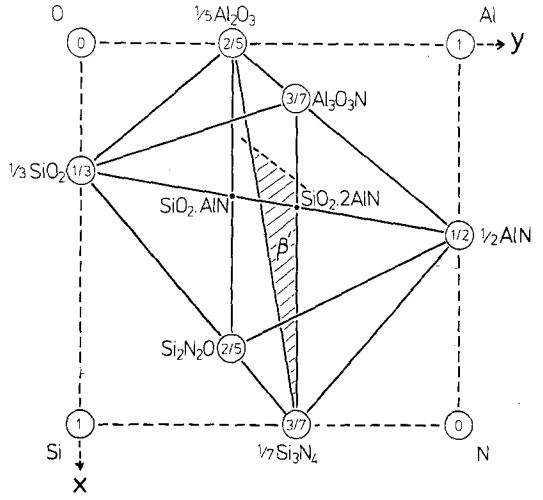

Figure 9 Irregular quadrilateral plane representing the Si_3N_4–AlN–Al_2O_3–SiO_2 system. Figures within circles are heights above the plane of the paper along the cube axis z. The shaded region, showing the supposed homogeneity limits of the β'-phase, is now known to be incorrect; see text.

the corners of which represent (1/7) Si_3N_4, (1/2) AlN, (1/5) Al_2O_3 and (1/3) SiO_2. The simplest representation is obtained by expressing concentrations in equivalents and, just as in a reciprocal salt pair (see Zernike [19]), the composition of any mixture can be characterized by two quantities

$$\frac{[\mathrm{Al}].3}{[\mathrm{Si}].4 + [\mathrm{Al}].3} \text{ and } \frac{[\mathrm{O}].2}{[\mathrm{N}].3 + [\mathrm{O}].2}.$$

When these ratios are plotted perpendicular to each other a square is obtained; see Fig. 10. It is convenient to let the bottom left-hand corner of the square represent 1 mol of Si_3N_4; the other three corners then represent Al_4N_4, Al_4O_6 and Si_3O_6 as in Fig. 11. It should be noted that all possible phases or mixtures of phases in which the combining elements Si, Al, O and N have their normal valencies lie within this diagram. It is the same as the irregular quadrilateral plane of Fig. 8 except that concentrations are expressed in equivalents instead of atomic units. Any point in the square of Fig. 10 or Fig. 11 is a combination of 12+ve and 12−ve valencies, i.e. it is convenient to regard compounds in ionic terms even though the interatomic bonding is predominantly covalent. In going from the left-hand to the right-hand side of the diagram, $3Si^{4+}$ is gradually replaced by $4Al^{3+}$; and from bottom to top, $4N^{3-}$ is replaced by $6O^{2-}$. The centre of the square represents a composition $Si_{1.5}Al_2O_3N_2$; note that the number of atoms changes with change in

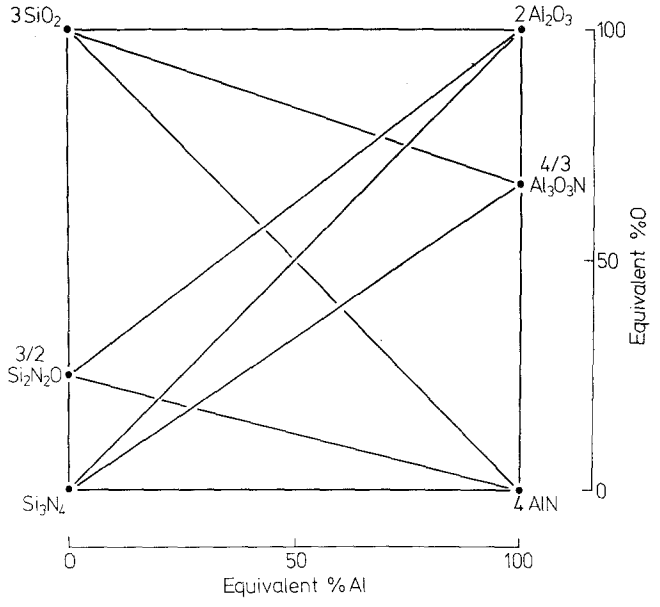

Figure 10 The square representation of the Si–Al–O–N system using equivalent concentrations.

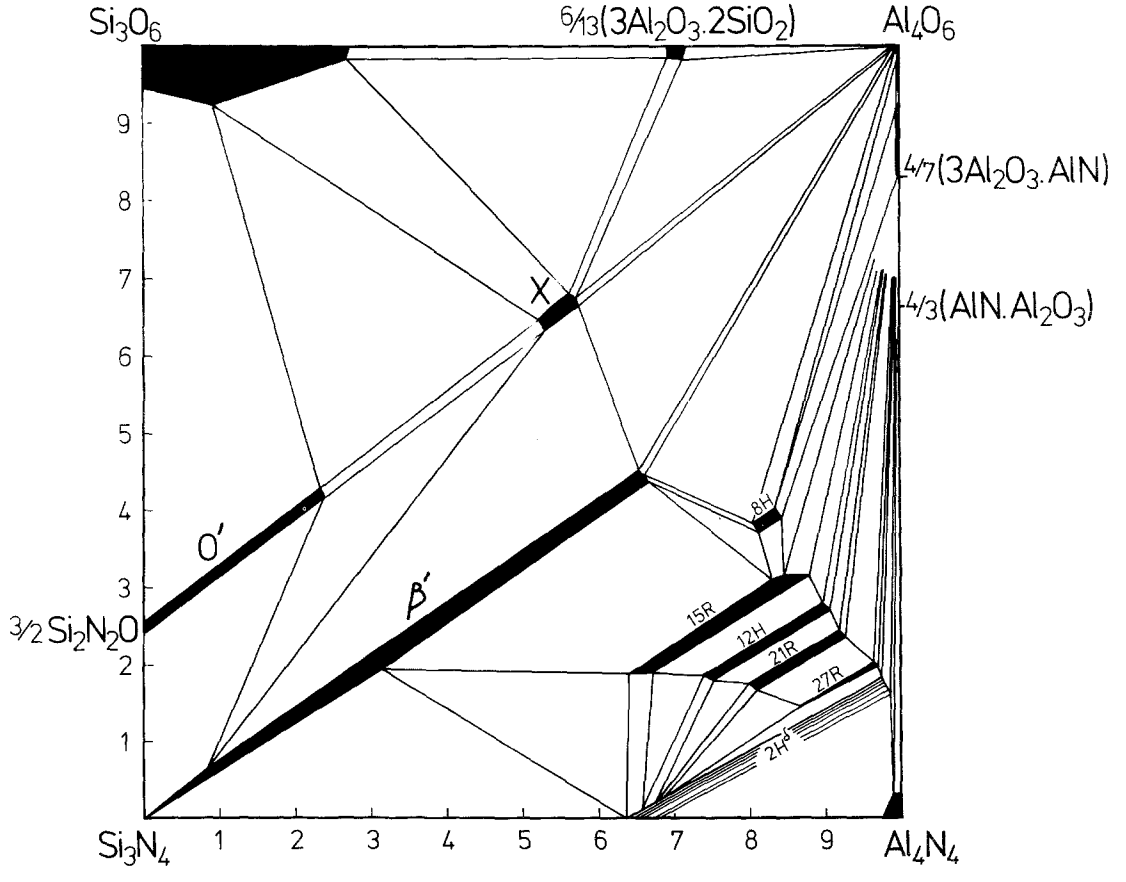

Figure 11 The Si_3N_4–AlN–Al_2O_3–SiO_2 system based on research at Newcastle.

position but the number of equivalents remains constant. Because of the constant $12^+:12^-$ "composition" it is often convenient to scale the sides of the square 0–12; each unit is then one valency.

In the Mg–Si–Al–O–N, Li–Si–Al–O–N and Y–Si–Al–O–N systems discussed below it is unlikely that any solid phases, vitreous or crystalline, contain atoms of variable valency and so each is what Zernike describes [19] as a "Quaternary system of the third kind". This is represented by Jänecke's triangular prism [20] in which all edges are equal. Fig. 12 outlines this representation for the magnesium–sialon system;

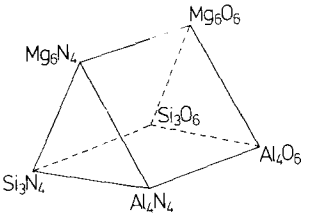

Figure 12 Outline representation of the magnesium–sialon system.

it is based on the standard Si_3N_4–Al_4N_4–Al_4O_6–Si_3O_6 square with Mg in equivalent units along a third dimension. The front triangular face of the prism represents nitrides and the rear face oxides. As shown below, each of the phases of the basal square plane extend into the prism volume and can often be represented on planes of constant M/X value which are not, of course, parallel with any of the prism faces and which cut other triangular planes representing pseudo-ternary systems e.g. $6MgO–Si_3N_4–4AlN$.

Although phase relationships in these sialon systems are often complicated, the adoption of the above representations has led to a much better understanding and interpretation of experimental observations. For ease of comparison it is suggested that other workers might use the same conventions.

4. The Si–Al–O–N system

The results of hot-pressing appropriate mixtures of Si_3N_4, AlN, Al_2O_3, SiO_2 and Si_2N_2O at high temperature in a graphite die are shown by Fig. 11 Hot-pressing was usually at 1750° C but higher and lower temperatures (1550–2000° C) were also employed. As far as possible, the same product was synthesized from different mixtures to check compositions and reproducibility. Thus, a mixture $4AlN:3SiO_2$ should give the same product as a mix $Si_3N_4:2Al_2O_3$. However, rates of reaction vary with different mixtures of the same total composition due to different particle sizes and different degrees of dispersion of one phase in another; the free energy change of the reaction also changes with different starting materials. At best, Fig. 11 is, therefore, an idealized behaviour diagram and does not necessarily represent thermodynamic equilibrium.

Each of the phases extends along a direction of constant M/X ratio whereas its homogeneity range in other directions is small. The similarity in the bond lengths Si–N (1.75 Å) and Al–O (1.75 Å) and the dissimilarity between Al–N (1.87 Å) and Si–O (1.62 Å) offers some explanation for this.

4.1. The β′-sialon phase

The β′ silicon nitride-type structure extends essentially along the 3M/4X line with a homogeneity range $Si_{6-z}Al_zO_zN_{8-z}$ where z reaches a maximum of about 4.2. The variation of the hexagonal unit-cell dimensions is shown by Fig. 13

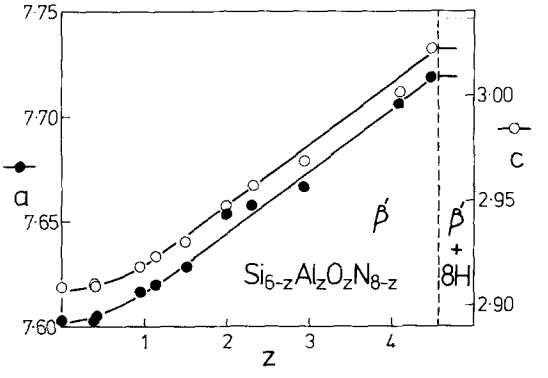

Figure 13 Unit-cell dimensions of β′-sialon.

Reaction of silicon nitride and alumina usually gives β′ and the silica-rich X-phase but the amount of the latter decreases as the hot-pressing temperature is increased above 1800° C. This accounts for the single-phase β′ products shown in Fig. 5 and is due to the loss of silica according to reactions (i)–(iii).

4.2. The O′-sialon phase

Silicon oxynitride reacts with alumina to extend along the 2M/3X join giving sialons with the Si_2N_2O-type structure and slightly larger unit-cell dimensions. As with β′, it can be prepared from a variety of oxide-nitride mixtures.

4.3. X-phase

The phase "X"–so-called because it could not at first be characterized–is identical with phase II reported by Oyama and Kamigaito [14, 21] who gave it the composition $3Al_2O_3 \cdot 2Si_3N_4$. It is usually the minor constituent which occurs in the production of β' from mixtures of silicon nitride and alumina and has also been variously designated as "Oyama-phase" and "J-phase". Its X-ray and electron diffraction patterns have been interpreted in terms of several different unit cells. For example Drew and Lewis [22] claim a triclinic structure with cell dimensions

$$\mathbf{a} = 9.9, \mathbf{b} = 9.7, \mathbf{c} = 9.5\,\text{Å},$$
$$\alpha = 109^\circ\ \beta = 95^\circ\ \gamma = 95^\circ$$

while Gugel *et al.* propose an orthorhombic lattice with

$$\mathbf{a} = 7.85, \mathbf{b} = 9.12, \mathbf{c} = 7.965.$$

Neither these nor other suggestions are compatible with the X-ray data obtained from specimens of at least 95% purity prepared at Newcastle. The composition is more Al_2O_3-rich than the original proposal [6] $SiAlO_2N$, and the unit cell has been determined [24] unequivocally as monoclinic with dimensions:

$$\mathbf{a} = 9.728, \mathbf{b} = 8.404, \mathbf{c} = 9.572\,\text{Å}, \beta = 108.96^\circ.$$

A complete structure determination is proceeding and although not yet complete it suggests that the initial description of X-phase as a "nitrogen-mullite" is not too misleading. Table III compares the observed low-angle X-ray data for X-phase with those calculated on the basis of these proposed dimensions.

TABLE III Observed and calculated X-ray data for X-phase; monoclinic with $\mathbf{a} = 9.728$, $\mathbf{b} = 8.404$, $\mathbf{c} = 9.572$ Å, $\beta = 108.96^\circ$

Indices	Interplanar spacing, d		Intensity
hkl	obs	calc	obs
1 0 0, 0 0 1	9.045	9.200, 9.052	vvw
1 0 $\bar{1}$	7.861	7.853	ms
1 0 1	5.602	5.606	ms
0 2 0	4.215	4.201	w
2 1 $\bar{1}$	4.167	4.152	w
0 1 2	3.982	3.985	mw
2 0 $\bar{2}$	3.926	3.927	mw
1 2 0	3.825	3.821	vw
2 0 1	3.649	3.650	s
1 0 2	3.621	3.622	vs
2 1 1	3.343	3.348	vvw
3 0 $\bar{1}$	3.243	3.242	vw
$\bar{1}$ 0 3	3.174	3.191	w
1 2 $\bar{2}$	3.139	3.136	vvw
3 0 $\bar{2}$	3.039	3.038	mw
0 0 3, 2 0 $\bar{3}$	3.013	3.017, 3.011	m
1 1 $\bar{3}$	2.984	2.983	vvw
2 0 2, 0 3 0	2.803	2.803, 2.801	ms
1 1 2	2.746	2.743	vvw
1 3 0, 0 3 1	2.680	2.679, 2.676	vvw
2 1 2, 3 0 1	2.653	2.659, 2.654	w
1 0 3, 3 0 $\bar{3}$	2.619	2.626, 2.618	m
1 1 3, 1 3 1	2.505	2.506, 2.505	s

TABLE IV Tetrahedral AlN-polytypes in the Si–Al–O–N system

M/X	type	a	c	c/n
4/5	8H	2.988	23.02	2.88
5/6	15R	3.010	41.81	2.79
6/7	12H	3.029	32.91	2.74
7/8	21R	3.048	57.19	2.72
9/10	27R	3.059	71.98	2.67
> 9/10	$2H^\delta$	3.079	5.30	2.65
1/1	2H	3.114	4.986	2.49

4.4. The tetrahedral AlN-polytype structures

Of the six uncharacterized phases reported by Gauckler *et al.* [16], the one which occurs most frequently is found as a minor phase in the hot-pressing of AlN-rich β' compositions; it was designated initially at Newcastle as "Y" and occurs also in the Mg–Si–Al–O–N system [25]. Electron micrographs show it as long laths similar to the morphology of α-SiC in a β-SiC matrix. Y-phase has now been identified [18] as rhombohedral with dimensions

$$\mathbf{a} = 14.045\,\text{Å}, \alpha = 12.30^\circ$$

corresponding to the hexagonal cell

$$\mathbf{a} = 3.010, \mathbf{c} = 41.81\,\text{Å}$$

and simply related to the wurtzite-type AlN structure of dimensions

$$\mathbf{a} = 3.114, \mathbf{c} = 4.986\,\text{Å}$$

In Ramsdell notation (see Parthé [26]) Y-phase is a 15R polytype of AlN and the other phases (see Fig. 11) are similarly identified as 8H, 12H, 21R and 27R. As shown in Table IV, which lists typical unit-cell dimensions, each type has a specific M/X composition ratio. Along the c-dimension the structure consists of "n" layers where "n" is the numeral of the Ramsdell symbol. The nR polytypes consist of three rhombohedrally related blocks each of $n/3$ layers, while the hexa-

gonal nH polytypes consist of two blocks related by a c-glide plane and each containing $n/2$ layers. Thus, the number of layers per symmetry-related block in the five polytypes

8H 15R 12H 21R and 27R

is respectively

4 5 6 7 and 9

corresponding to the following M/X ratios

4/5 5/6 6/7 7/8 and 9/10

The 2H AlN structure (see Fig. 14) with M/X = 1/1 is the end member of this series but a similar 2H structure with an expanded c-dimension is obtained at M/X ratios greater than 9/10 but less than 1/1. The systematic variation of unit-cell dimensions with polytype number is shown by Fig. 15 in which the c-dimension can be expressed in Ångstroms as

$$c_n = (n-3)\,2.493 + 3(4.014)$$

and

$$c_n = (n-2)\,2.493 + 2(4.014)$$

for respective rhombohedral and hexagonal structures of compositions

$$M/X = n/n+3 \text{ and } M/X = n/n+2.$$

The increase in the effective layer-spacing from 2.493 to 4.014Å in one layer of each block is due to an extra non-metal atom X which also causes a change in the stacking sequence. In a close-packing of n metal atoms there are $2n$ tetrahedral sites the apices of n of which point upwards while the other n tetrahedra point downwards. The centres of these tetrahedra are possible sites for non-metal atoms X and are directly above and below each metal atom with an M-X distance equal to three-quarters of the layer spacing. Occupation of half the number of tetrahedra, for example all those pointing upwards as in AlN, gives a composition MX. Occupation of all tetrahedra, giving a composition MX_2, requires tetrahedra above and below each other to share a common face and gives an impossibly short distance between non-metal atoms equal to

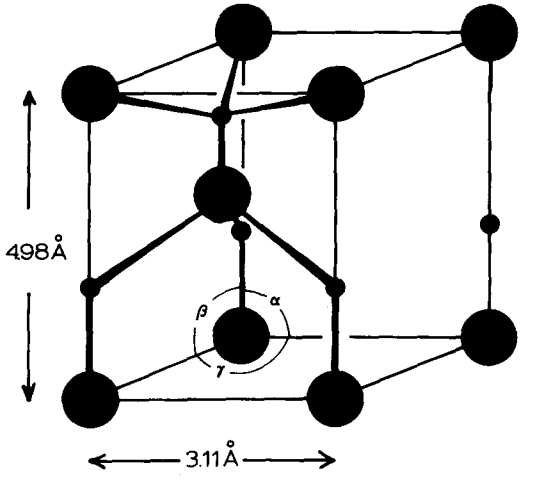

Figure 14 The 2H AlN structure.

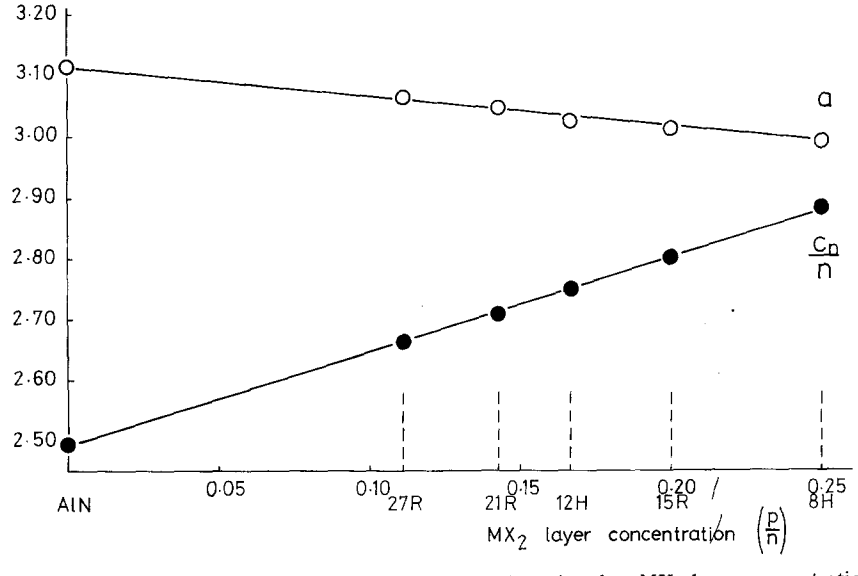

Figure 15 Unit-cell dimensions of defect AlN-polytype sialons plotted against MX_2 layer concentration.

half the layer spacing, i.e. not more than about 2.0 Å in the AlN polytypes. If, however, all tetrahedra in only one layer are occupied and adjacent layers only half-occupied, the tetrahedra in neighbouring layers avoid sharing a common face if the stacking sequence of the metal-atom layers is changed locally from close-packed hexagonal ABAB . . . to face-centred cubic ABC . . . .

The metal-atom packing and the sequence of half-filled (X) and completely filled (XX) tetrahedra in the 8H polytype are thus:

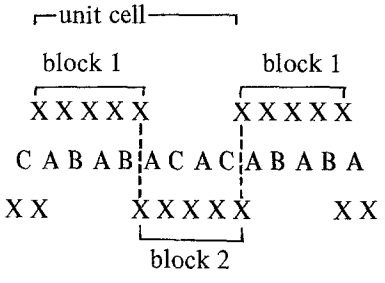

It follows that polytypes with n even are hexagonal and those with n odd are rhombohedral. Idealized projections of the 15R and 12H unit cells on the (1 1 0) plane are shown by Fig. 16 and the X-ray data for 15R are listed in Table V. The expanded 2H polytype must also be a defect structure but the concentration of additional non-metal-atoms is too small for an ordered arrangement and so the phase is designated $2H^{\delta}$

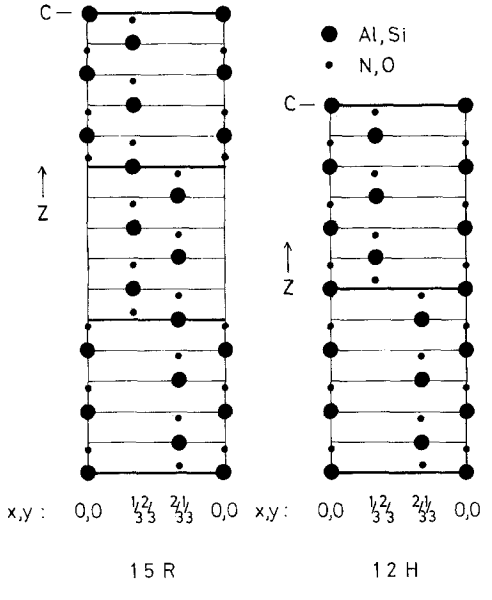

Figure 16 Projections of the 15R and 12H structures on the (1 1 0) plane.

TABLE V X-ray data for the 15R AlN-polytype sialon structure (Y-phase sialon)

hkl	d_{calc}	d_{obs}	I
0 0 3	13.950	13.990	w
0 0 1 5	2.787	2.784	s
1 0 1	2.602	2.602	s
0 1 2	2.587	2.587	ms
1 0 4	2.529	2.520	w
0 1 5	2.489	2.488	ms
1 0 7	2.389	2.389	s
0 1 8	2.333	2.333	mw
0 0 1 8	2.323	2.323	mw
1 0 1 0	2.212	2.212	mw
0 1 1 1	2.150	2.149	m
0 0 2 1	1.991	1.990	w
0 1 1 4	1.964	1.960	mw
1 0 1 6	1.845	1.845	ms
0 1 1 7	1.789	1.785	ms

Hexagonal **a** = 3.010, **c** = 41.81 Å
Rhombohedral **a** = 14.04 Å, $\alpha = 12.3°$

where δ indicates disorder in the sequence of MX_2 layers. The effective spacing (4.014 Å) between metal atoms in MX_2 layers where all tetrahedra are occupied is, as might be expected, much larger than that for a MX layer (2.493 Å). The proposed structures account for the measured densities of the specimens and for the main features of the X-ray data but they are undoubtedly idealized models and further work on structure refinement is now proceeding. They represent a new kind of polytype the structure of which is determined by the metal:non-metal atom-ratio.

The homogeneity limits of the phases undoubtedly vary with temperature. It has been shown [18], for example, that the phase designated by Lejus [27] as "X" occurring in the Al_2O_3–AlN system at above 1800°C has a 21R structure. Although the composition of "X" is given as near $Al_5O_3N_3$ its structure now suggests M_7X_8. It seems that at higher temperatures the 21R sialon phase field shown in Fig. 11 extends as far as the Al_4N_4–Al_4O_6 join.

4.5. The technological significance of the AlN–polytype sialons

It is shown below that the AlN–polytype phases appear in the magnesium and lithium sialon systems. Aluminium nitride is itself a candidate for high-temperature engineering applications and it has been shown by Komeya *et al.* [28] that the desirable fibrous microstructures formed in the AlN–Y_2O_3 system are associated with a silica impurity. The published X-ray diffractometer

patterns show major amounts of what is described as a pseudo-hexagonal "Al–Si–O–N" phase in mixtures of $85AlN–5Y_2O_3–10SiO_2$ and $80AlN–10Y_2O_3–10SiO_2$ sintered at 1800°C in nitrogen. We have identified the four most intense peaks as reflections from an AlN–polytype with an M/X ratio of about 9/10.

Umebayashi and Kobayashi have recently reported [29] the formation of β'-sialon and an unknown phase as a product of sintering a mixture of volcanic ash and aluminium powder in nitrogen at 1400°C. With 50 wt% aluminium the unknown phase is the major component; its quoted d values of 2.795, 2.605, 2.493, 2.396, 2.331 and 2.154 Å correspond with the strongest X-ray reflections of the 15R (Y-phase) polytype listed in Table V.

The relationship between mechanical properties and the microstructure of nitrogen ceramics is not known in detail but it is suggested [28] that a fibrous morphology (such as that of the AlN–polytypes) is advantageous.

A composite of $\beta' + 15R$ sialons can be readily produced as a pseudo-equilibrium mix (see Fig. 11) and its fracture toughness might well be better than that of pure homogeneous β'. The control of microstructure is one of the most important requirements in sialon development.

4.6. Liquids, glasses, and other crystalline phases

X-phase melts at above about 1650°C and so at 1750°C much of the region of Fig. 11 between O′, X and Si_3O_6 is liquid. On cooling, O′, X and β' crystallize but some glass is always retained. In the area between O′ and Si_3O_6, increasing amounts of glass are formed as the silica content increases until at about half-way towards the Si_3O_6 corner a homogeneous nitrogen-containing vitreous phase can be obtained by cooling in the hot-press from 1600°C.

With compositions between X-phase and the Al_4O_6 corner of the Si–Al–O–N diagram hot-pressing at 1450 to 1500°C gives products containing yet another new phase the diffraction pattern of which has not been interpreted.

5. Properties of β'-sialons

β' has been the only sialon so-far examined in any detail and because, until recently, specimens usually contained other vitreous or crystalline phases (e.g. X or 15R) it is not certain whether the intrinsic properties of β' have yet been evaluated. Even with such limitations the results are promising for a variety of applications. Most measurements are on compositions containing about equal concentrations of silicon and aluminium, i.e. $Si_3Al_3O_3N_5$ with $z = 3$. Because of its structure, its physical and mechanical properties are similar to those of β-silicon nitride, but chemically it is closer to aluminium oxide. Thus (see Fig. 17), its thermal expansion co-

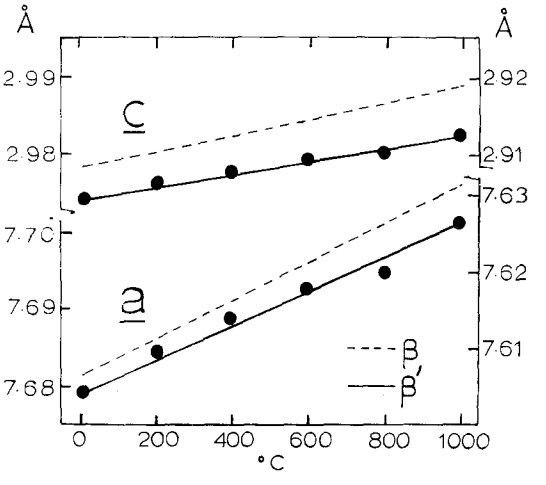

Figure 17 Thermal expansion of β'-sialon ($z = 3$; full lines) compared with β-Si_3N_4 (dashed lines).

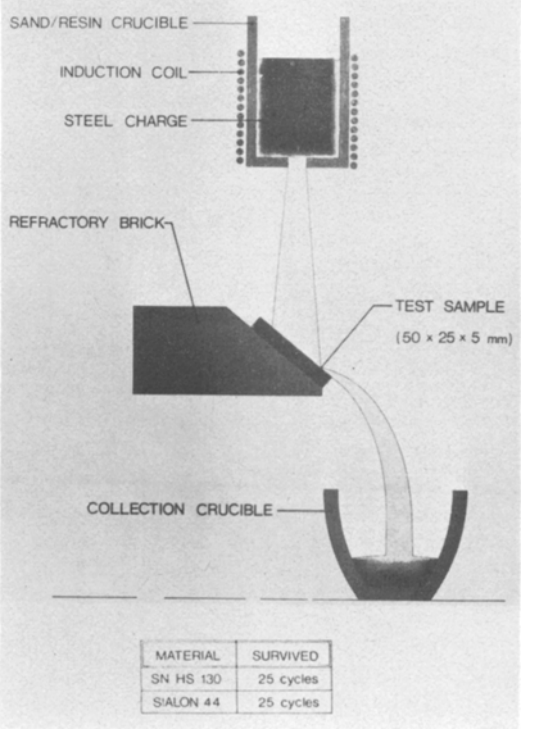

Figure 18 Joseph Lucas Limited steel splash test [30].

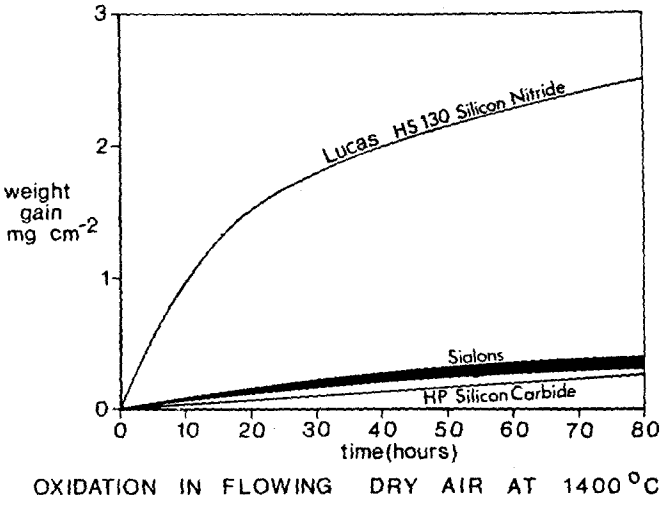

Figure 19 Oxidation in flowing dry air at 1400° C of silicon nitride, β'-sialon and silicon carbide [30].

efficient (2.7×10^{-6}) is less than that of β-Si_3N_4 (3.5×10^{-6}) and so its thermal shock properties are at least as good as hot-pressed silicon nitride (Fig. 18). Oxidation resistance (see Fig. 19) is better than for silicon nitride, probably because a coherent and protective layer of mullite is formed on the surface. Compatability with molten metals is surprisingly good and the buttons shown in Fig. 20 were kept molten in sialon crucibles for 30 min – aluminium and copper at 1200°C and pure iron and cast iron at 1600°C; neither the metals nor the crucibles showed signs of attack. Larger scale tests made by Joseph Lucas Limited are shown by Fig. 21.

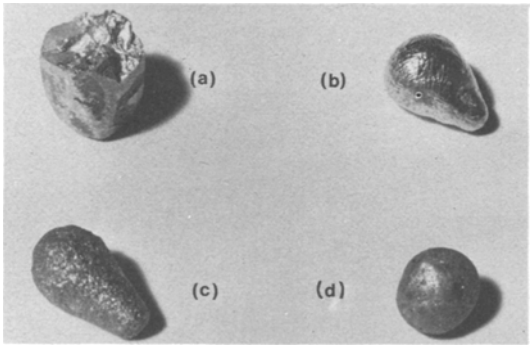

Figure 20 Compatibility of sialon crucibles with molten metals: (a) aluminium; (b) copper; (c) pure iron; (d) cast iron.

The use of sialons for holding and conveying molten metals, including steel, is perhaps more important – and more easily realized – than the very exacting applications for turbine blades.

One potential advantage of sialon over silicon nitride is in fabrication. The usual ceramic techniques of extrusion, pressing and slip-casting can be used to produce shapes of the mixed components and then these can be fired to near-theoretical density in an inert atmosphere at about 1600° C. As will be shown later, densifying agents which promote liquid-phase sintering can subsequently be incorporated in the sialon structure.

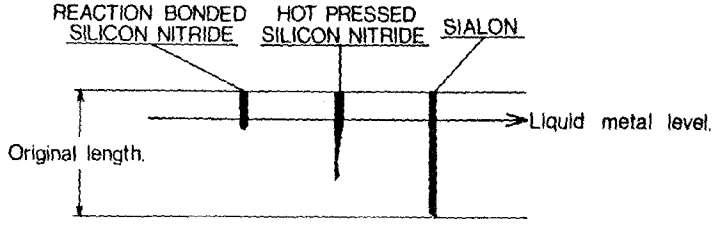

STEEL	TEMP °C	TIME min	% Wt Loss		
			RBSN	HPSN	SIALON
MILD STEEL	1650	25	100	84	5
STAINLESS STEEL	1600	15	100	17	5

Figure 21 Resistance of sialon and silicon nitride to attack by molten steel [30].

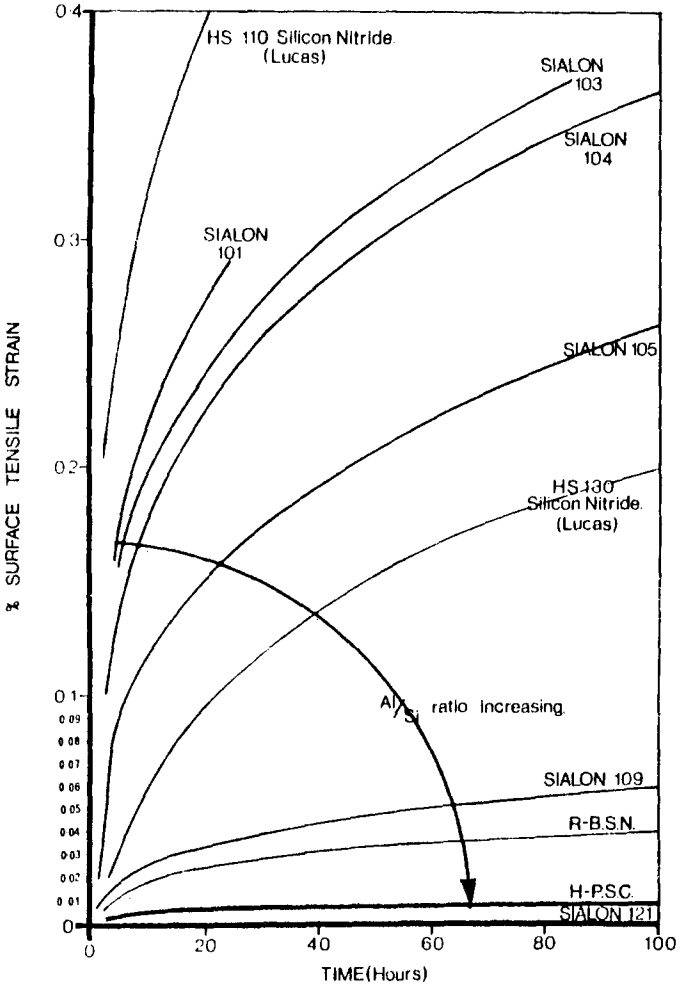

Figure 22 Creep of silicon nitride, silicon carbide and various sialons at 1225° C and 11,000 psi; after Joseph Lucas Limited [30].

With a reliable behaviour diagram for the Si–Al–O–N system (Fig. 11) it is now possible to produce β'-phase or ($\beta' + 15R$) mixed-phase sialons free from glass and because the creep of nitrogen ceramics is essentially related to their glass content, the glass-free materials are highly creep-resistant. The creep behaviour of sialons with varying Al/Si ratio (see Fig. 22) is thus explained.

6. Metal-sialon systems

Magnesium, manganese, lithium and other metal–silicon nitrides and oxynitrides all have structures based on that of aluminium nitride (see Fig. 14). AlN is built up of AlN_4 tetrahedra; in $MgSiN_2$ there are equal numbers of MgN_4 and SiN_4 tetrahedra; and in $LiSi_2N_3$ there are twice as many SiN_4 tetrahedra as LiN_4 units. Fig. 23 and Table VI show that the structures can be regarded as orthorhombic superlattices of the hexagonal AlN. It seemed likely, therefore, that these

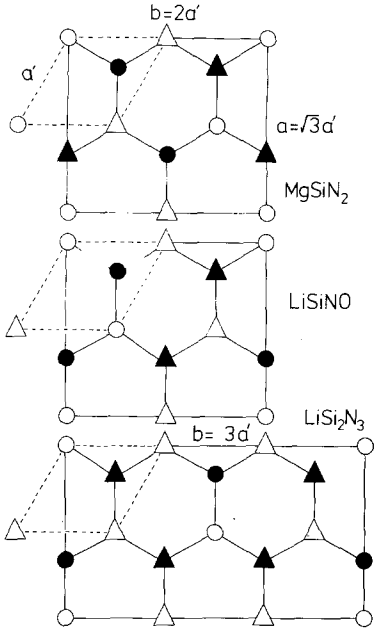

Figure 23 Typical metal–silicon nitride and oxynitride structures.

TABLE VI Orthohombic unit-cell dimensions of some wurtzite-type structures

	$a = \sqrt{3}a'$	$b = 2a'$	$c = c'$
AlN	5.39	6.22	4.98
$MgSiN_2$	5.275	6.455	4.978
LiSiNO	5.194	6.394	4.742
Li_2SiO_3	5.395	9.360	4.675
$LiSi_2N_3$	5.303	9.196	4.780
Si_2N_2O	5.498	8.877	4.853
$(Si, Al)_2(O, N)_3$	5.498	8.913	4.856
		$b = 3a'$	

metals Mg, Mn, Li and perhaps others could be incorporated into sialons.

6.1. The Mg–Si–Al–O–N system

As shown by Fig. 6, magnesium spinel, $MgAl_2O_4$, or equimolecular mixtures of MgO and Al_2O_3 react with silicon nitride to give β'-magnesium sialons retaining the M/X ratio of 3/4. Preliminary observations have been reported [25] but their interpretation requires revision in the light of more recent investigations [31]. For example, phases initially designated "Y" and "Q" in the system are now recognised as 15R and 12H polytypes. In general, the phases which occur in the basic Si–Al–O–N system extend into the Mg–Si–Al–O–N prism (Fig. 12) to a greater or less extent but other new phases are also found. The $MgO–Si_3N_4–Al_2O_3$ section, represented in Fig. 24 by an equilateral triangle, cuts across planes of constant M/X ratio and so includes few single-phase regions; these occur at compositions represented in other sections of the large volume. In addition to β' occurring along the $Si_3N_4–MgAl_2O_4$ join, phases α' (isostructural with α-silicon nitride), X, 12H, 15R and a nitrogen spinel are observed. The homogeneity range of the nitrogen-spinel is fairly extensive and is shown better by the Mg–Al–O–N prism-face of Fig. 25.

The polytype 21R accommodates negligible concentrations of magnesium but "R"-phase, although shown as being on the AlN–MgO join, has either a $2H^{\delta}$ or a 27R structure according to its unit-cell dimensions. The X-ray reflections are broad and somewhat diffuse suggesting a range of homogeneity and, as in all preparations involving magnesium and nitrogen at high temperatures,

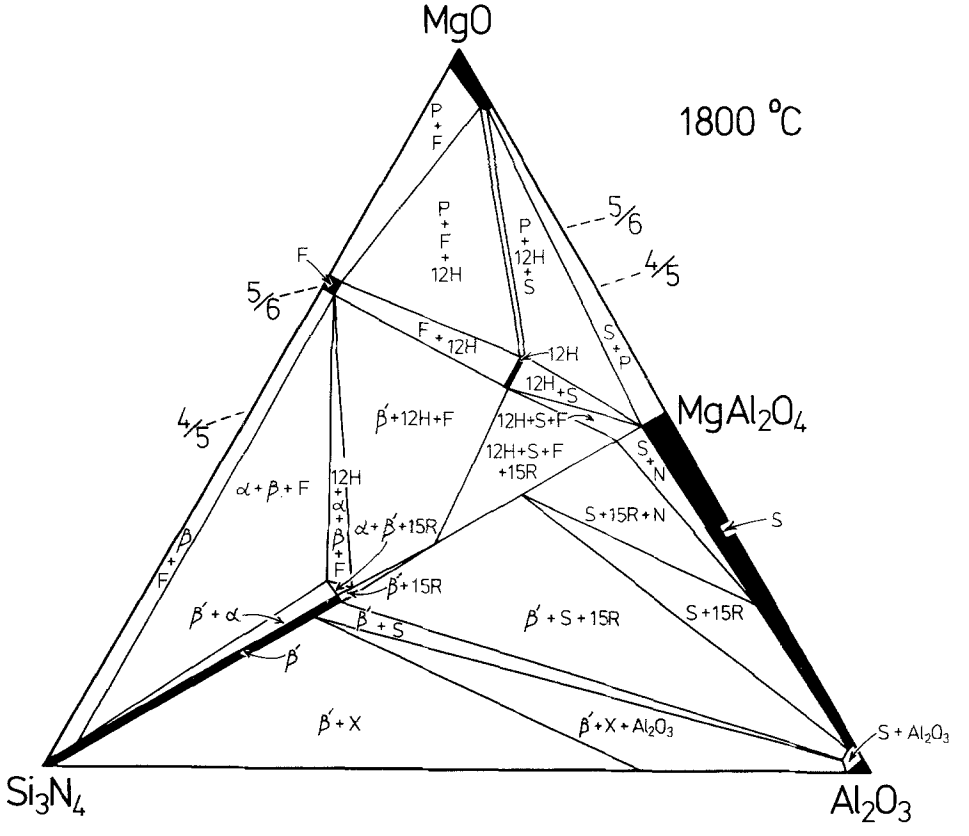

Figure 24 The $MgO–Si_3N_4–Al_2O_3$ section of the Mg–Si–Al–O–N system at 1800° C.

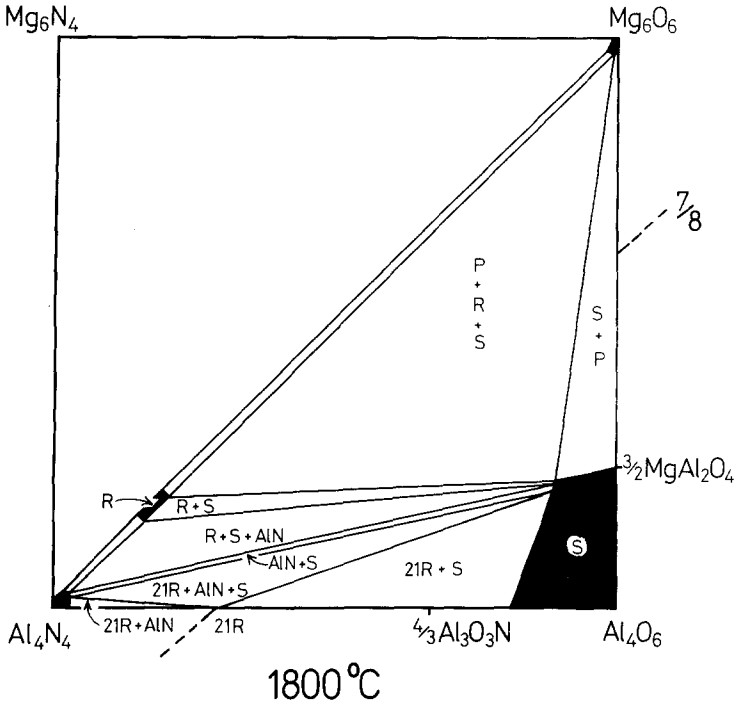

Figure 25 The Mg–Al–O–N prism-face of the Mg–Si–Al–O–N system at 1800° C.

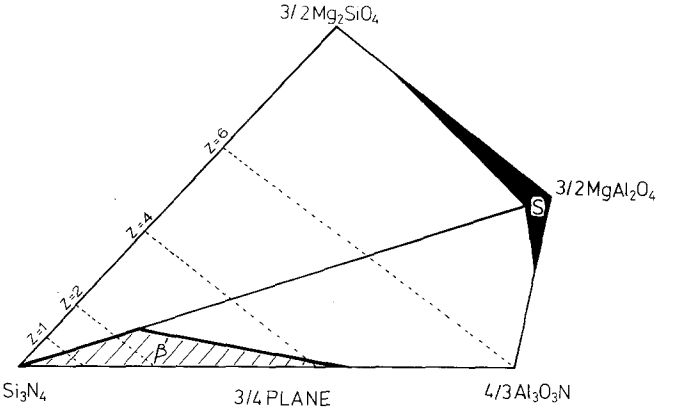

Figure 26 The 3M/4X plane of the Mg–Si–Al–O–N system at 1800° C.

there is every probability of losing Mg_3N_2 by volatilization; this would reduce the M/X ratio from its initial value of 1/1. A feature of the Mg–Si–O–N subsystem is the occurrence of liquid phases which, on cooling, produce nitrogen glasses.

The 3M/4X plane of the system (see Fig. 26) is important in showing that the β'-sialon extends along this plane from the Si_3N_4–Al_3O_3N join towards forsterite, Mg_2SiO_4. Silicon nitride always contains silica as a surface layer and this, as previously stated, prevents the production of homogeneous, single-phase hot-pressed material. By addition of appropriate amounts of Al_2O_3 and AlN together with just sufficient MgO to react with the surface silica, a homogeneous β'-magnesium sialon can be obtained. Moreover, the magnesium silicate reacts first with some silicon nitride to produce a liquid which aids densification by liquid-phase sintering, and then, by suitable heat-treatment, it is possible to incorporate this in solid solution to give the single-phase β'.

6.2. The Li–Si–Al–O–N system

Lithium–silicon nitride $LiSi_2N_3$ and silicon oxynitride Si_2N_2O are essentially isostructural (see Table VI and Fig. 27) in which the latter

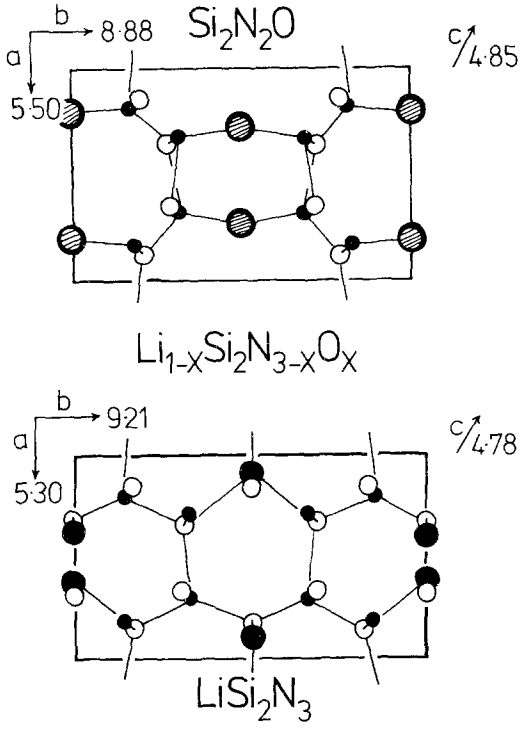

Figure 27 The $LiSi_2N_3$ and Si_2N_2O structure.

TABLE VII Possible reactions in the Li–Si–Al–O–N system

(1) $LiSi_2N_3 \rightarrow Li_{1-x}Si_2N_{3-x}O_x \rightarrow Si_2N_2O$
(2) $LiSi_2N_3 \rightarrow Li_{1-y}Si_{2-y}N_{3-3y}O_{3y} \rightarrow Li_2SiO_3$
(3) $Si_2N_2O \rightarrow Si_{2-z}Al_zN_{2-z}O_{1+z} \rightarrow Al_2O_3$

is obtained from the former by replacing one nitrogen atom by oxygen and, at the same time, satisfying valency requirements by replacing the lithium with a vacancy. Indeed, preparations of "$LiSi_2N_3$" usually contain oxygen and are lithium deficient, $Li_{1-x}Si_2N_{3-x}O_x$. More extensive solid solubility seemed likely and other possibilities, occurring separately or simultaneously, are given in Table VII. As with the magnesium sialons, completely new phases occur in the Li–Si–Al–O–N system as well as those which extend from the basic Si–Al–O–N behaviour diagram. Reaction of silicon nitride with lithium–aluminium spinel, $LiAl_5O_8$ gives a β'-lithium sialon and with lithium aluminate, $LiAlO_2$, a sialon (α') with the structure of α-silicon nitride.

Other nitrogen-containing phases have structures based on β-eucryptite (Eu'), spinel (S),

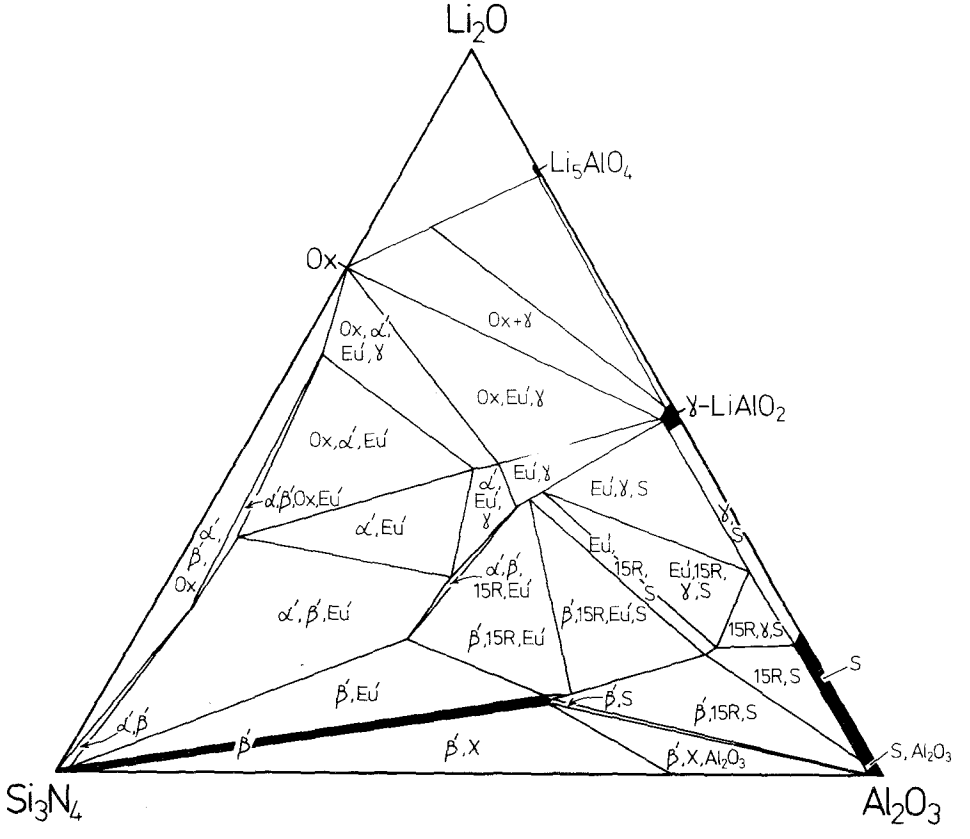

Figure 28 The Li_2O–Si_3N_4–Al_2O_3 section of the Li–Si–Al–O–N system at 1550° C.

silicon oxynitride (O′ or Ox), tetragonal cristobalite (γ) and the polytype 15R. The section Li_2O–Si_3N_4–Al_2O_3 of Fig. 28 shows these, but again there are no extensive single-phase regions. The variations of unit-cell dimensions observed in the multi-phase products show that each phase has a wide range of homogeneity even though it might be characterized by a specific M/X atom ratio.

Spinels in general react with silicon nitride to give β'-phases provided that the appropriate metal atoms can exist in four-fold co-ordination. Thus, manganese, zinc and cuprous spinels all give β'-sialons similar to the magnesium and lithium ones.

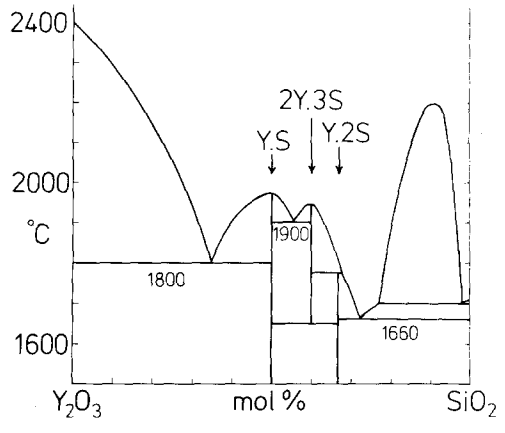

Figure 29 The Y_2O_3–SiO_2 system.

7. Yttrium sialons and the role of yttria in hot-pressing silicon nitride

The high-temperature strength and creep resistance of silicon nitride hot-pressed with MgO additive is impaired by the formation of a grain-boundary magnesium–silicon oxynitride glassy phase the softening temperature of which depends upon its impurity content, particularly calcium and other alkalis and alkali earths. Gazza [32] showed that improved properties were obtained by using yttria additions instead of magnesia, and suggested that these produced a more refractory grain-boundary phase. In the Y_2O_3–SiO_2 system (Fig. 29) the lowest liquid temperature is 1660°C. With up to 5 wt% Y_2O_3, yttrium silicates are indeed formed but consistent improvements in hot-strength were obtained with not less than about 15 wt% Y_2O_3 – much more than is required to react completely with the surface silica on silicon nitride powder. Moreover, other oxides giving silicates and eutectics with equally high melting temperatures were explored as additives but were found ineffective.

The unique role of yttria has been explained by work at Newcastle [33] which has since been extended to wider investigations of the Y–Si–O–N and yttrium–sialon systems [34].

7.1. The hot-pressing sequence

After hot-pressing at 1700°C and above, increasing amounts of glass are observed in the products

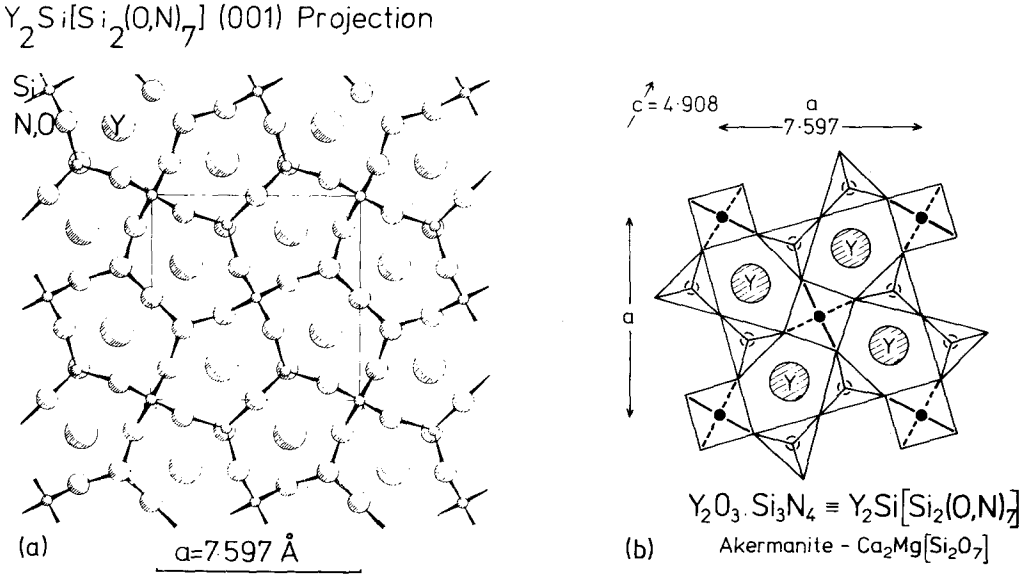

Figure 30 Projection of $Y_2Si[Si_2O_3N_4]$ on (0 0 1).

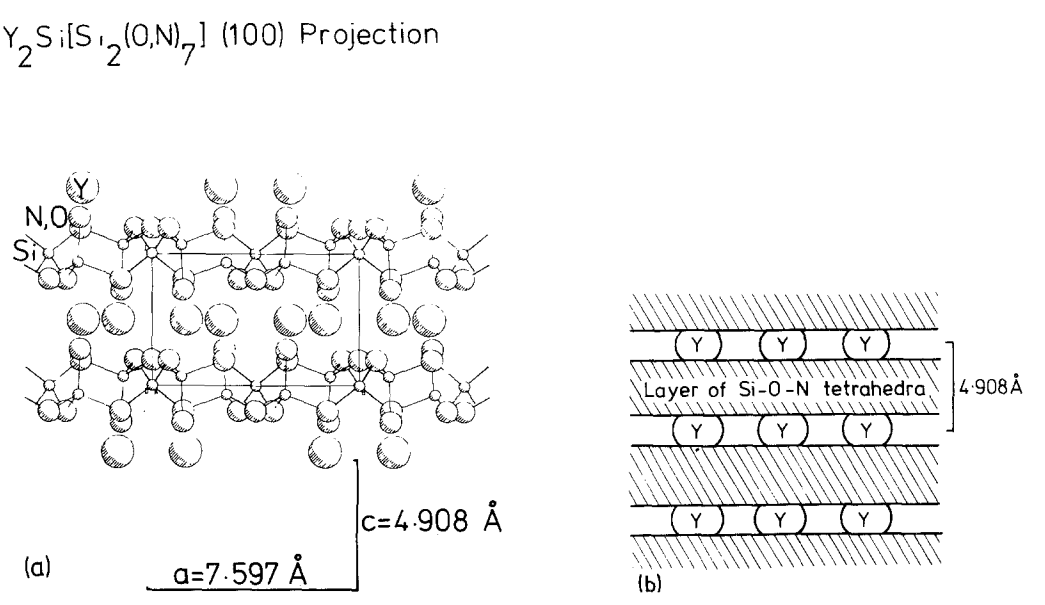

Figure 31 Projections of $Y_2Si[Si_2O_3N_4]$ on (1 0 0).

with up to 5 to 10 wt% Y_2O_3 but the glass then decreases and becomes negligible with 15 to 20 wt% yttria. Only β-Si_3N_4 and a new yttrium–silicon oxynitride $Y_2O_3 \cdot Si_3N_4$ are observed. At temperatures up to about 1800° C Y_2O_3 reacts with α-Si_3N_4 to give two further new phases, both yttria-rich and designated initially as "H" and "J". These melt below 1700° C and then react with more silicon nitride to give the $Y_2O_3 \cdot Si_3N_4$. The latter has the same tetragonal structure as Akermanite $Ca_2Mg[Si_2O_7]$ and Gehlenite $Ca_2Al[SiAlO_7]$, members of the melilite series of silicates. In the yttrium–silicon oxynitride, sheets of $Si(O_{0.4}N_{0.6})_4$ tetrahedra are stacked one on top of the other and are held together by yttrium ions between them; see Figs. 30 and 31. It forms a continuous series of solid solutions with both Akermanite and Gehlenite and the melting points of the 50:50 intermediates listed as (2) and (4) in Table VIII are above 1600° C. Thus, appreciable amounts of calcium, aluminium, magnesium and probably other impurities present in silicon nitride can be accommodated in the "Ysion" structure without any loss of refractoriness. In concurrent work Tsuge *et al.* [35] indexed the diffraction pattern of the oxynitride without determining its structure and report that it melts at 1825° C.

TABLE VIII Solid solution series in the nitrogen-melilites

Y-N melilites	
(1) Akermanite 1454° C	$Ca_2Mg[Si_2O_7]$
(2) (1) + (3)	$(Y, Ca)_2(Mg, Si)[Si_2O_5N_2]$
(3) "Ysion" $Y_2O_3 \cdot Si_3N_4$	$Y_2Si[Si_2O_3N_4]$
(4) (3) + (5)	$(Y, Ca)_2(Si, Al)[(Si, Al)_2O_5N_2]$
(5) Gehlenite 1590° C	$Ca_2Al[SiAlO_7]$

Yttria seems an ideal hot-pressing additive for silicon nitride because at lower temperatures it forms liquid phases which allow rapid sintering and then at higher temperatures when densification is complete these phases react with more silicon nitride to give a highly refractory bonding phase. There seems no reason why this kind of mechanism should not be equally effective in pressureless sintering.

Of greater importance in the characterization of the yttrium–silicon oxynitride, it is the first sialon with a layered structure similar to that of the sheet silicates. It suggests that nitrogen clays and micas, for example, might also exist.

7.2. Nitrogen apatites

The "H"-phase which precedes or accompanies the formation of the yttrium–silicon oxynitride during hot-pressing was identified [18] (see discussion of the paper by Rae *et al* [35]) as being isostructural with fluoro-apatite $Ca_5(PO_4)_3F$ and hydroxy-apatite $Ca_5(PO_4)_3OH$, the structural materials of bones and teeth. Table IX shows

TABLE IX X-ray data for nitrogen-apatite and an apatite-silicate

h k l	Spencite $Y_4Ca(SiO_4)_3O$		"H" ≡N–Apatite $Y_5(SiO_4)_3N$	
	d	I/I_0	*d*	I/I_0
1 1 0	–		4.69	vw
2 0 0	4.02	50	4.05	ms
1 1 1	3.83	40	3.86	mw
0 0 2	3.42	30	3.38	m
1 0 2	3.13	50	3.12	ms
2 1 0	3.05	40	3.08	m
2 1 1	2.78	100	2.80	vs
1 1 2	2.76	40	2.75	ms
3 0 0	2.69	30	2.71	ms
a	9.32		9.41	
c	6.84		6.76	

that the diffraction pattern and unit-cell dimensions of "H" are almost identical with those of Spencite, a yttrium–calcium silicate $Y_4Ca(SiO_4)_3O$ with an apatite structure. "H"-phase was therefore thought to be $Y_5(SiO_4)_3N$ with a hexagonal structure represented in Fig. 32.

Other nitrogen-apatites have recently been reported by Lang *et al.* from Rennes [36]. In the general formula $(Ln, M)_5Si_3(O, N)_{13}$:

Ln = La, Nd, Sm or Gd
M^{III} = Cr
M^{IV} = Ge, Sn or Mn
M^{V} = V
and M^{VI} = Mo.

When the metal M is trivalent the number of nitrogen atoms $N = 1$; for M^{IV}, $N = 2$; for M^{V}, $N = 3$; and for M^{VI}, $N = 4$. Our own most recent work shows that the Y:Si ratio is generally less and the nitrogen content is higher in the nitrogen–yttrium apatite than is represented by the composition $Y_5Si_3O_{12}N$ initially proposed. In fact, it has an appreciable homogeneity range near $(Y_4Si)(Si_3O_{11}N)N$. Clearly, nitrogen must occupy some of the corners of SiO_4 tetrahedra in addition to the special sites co-ordinated by the triangle of three Y atoms shown in Fig. 32; some Si must also replace Y. Much more detailed investigation is required, but the discovery of nitrogen-apatites opens up still further possibilities for nitrogen modifications of important structural materials.

7.3. The Y–Si–O–N system

The behaviour diagram of Fig. 33 deduced from pressings at 1600° C and 2600 psi for 1 h summarizes the most recent Newcastle work on the Y–Si–O–N system. In agreement with Fig. 29, the only yttrium silicates found at this temperature are Y_2SiO_5 and β-$Y_2Si_2O_7$ both of which are monoclinic. "J"-phase, which is found in silicon nitride hot-pressed with more than 5 wt% Y_2O_3 below 1700° C, has been reported by Tsuge *et al.* [35] as $Si_3N_4 \cdot 2Y_2O_3$ and by Wills [37] as $Si_3N_4 \cdot 3Y_2O_3$. Both are incorrect; it lies off the Si_3N_4–Y_2O_3 join with a composition $2Y_2O_3 \cdot Si_2N_2O$ and its X-ray diffraction pattern is similar to that of the yttrium aluminate $2Y_2O_3 \cdot Al_2O_3$ ("YAM"). In the latter, substitution of 2Al by 2Si and of 2O by 2N leads to the composition now proposed. Just as there is solid solu-

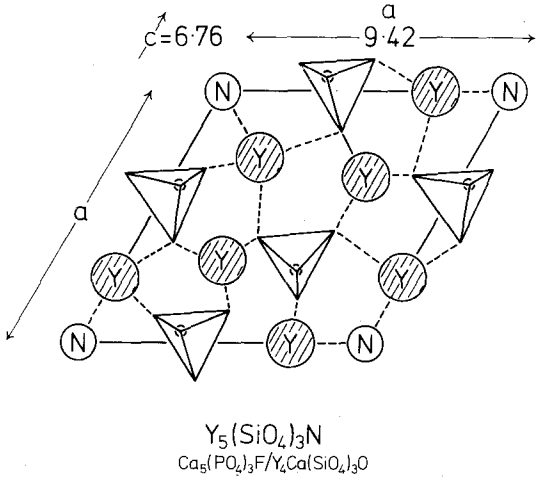

Figure 32 Projection on (0 0 1) of one-half of the unit-cell of nitrogen–yttrium apatite.

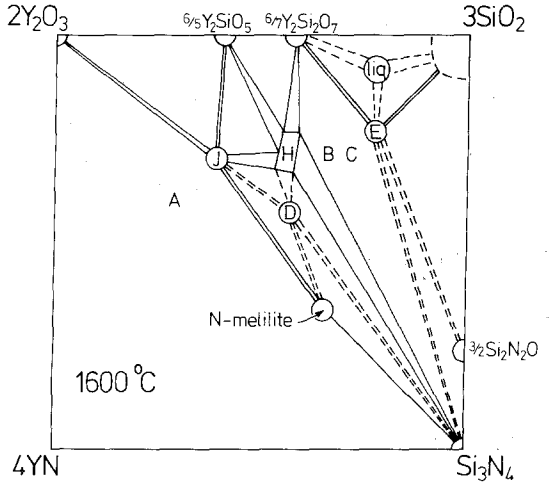

Figure 33 The Y_2O_3–YN–Si_3N_4–SiO_2 section of the Y–Si–Al–O–N system at 1600° C.

tion of alumina in silicon oxynitride, there is undoubtedly solid solution between "J" and "YAM" in the Y–Si–Al–O–N system.

In Fig. 33, "H"-phase is the nitrogen-apatite already discussed. "D" has a composition close to $YSiO_2N$ and a hexagonal structure not yet completely resolved. "E"-phase has a composition YSi_3O_6N; it is isostructural with β-$Y_2Si_2O_7$ and is derived from it by substitution of Y by Si and simultaneously of O by N.

The compositions and structures of the "A", "B" and "C" phases are not yet defined. The Y–Si–O–N behaviour diagram, although still far from completely or unequivocally established, offers explanations for some of the previously inexplicable observations of hot-pressing silicon nitride with yttria [32]. Since silica forms a surface layer on the nitride, reaction with yttria will locally give the liquid phase near the SiO_2 corner (see Fig. 33).

Eventually, as silicon nitride reacts, either N-apatite ("H") or N-melilite, or mixtures of these if the phase "D" is unstable above 1700° C, will form as a grain-boundary phase depending on how much silica is volatilized. The product will depend not only on the impurity content of the silicon nitride but also critically upon its initial silica content and the amount removed by reaction with graphite during the pressing.

8. Nitrogen glasses

In the hot-pressing of silicon nitride with magnesium oxide it has already been mentioned that a phase, liquid at high temperature, cools to give a glass. Fig. 34 from Nuttall and Thompson [38] shows a well-formed β-Si_3N_4 crystal which has nucleated and grown from the liquid. If the glass is merely a magnesium silicate with impurities, it would be expected from the MgO–SiO_2 phase diagram (Fig. 35) to devitrify giving enstatite and cristobalite. Instead, it gives [39] enstatite and silicon oxynitride (Si_2N_2O) after heat-treatment at 1350° C; see Fig. 36. Both the original high-temperature liquid and the glass which forms on cooling must, therefore, contain nitrogen.

Bulk samples of this nitrogen-glass have been obtained by both hot-pressing and by pressureless heat-treatment in a boron nitride crucible of mixtures of MgO, SiO_2 and Si_3N_4 at 1700° C. Without silicon nitride, mixtures of 20 wt% MgO : 80 wt% SiO_2 give a product showing only

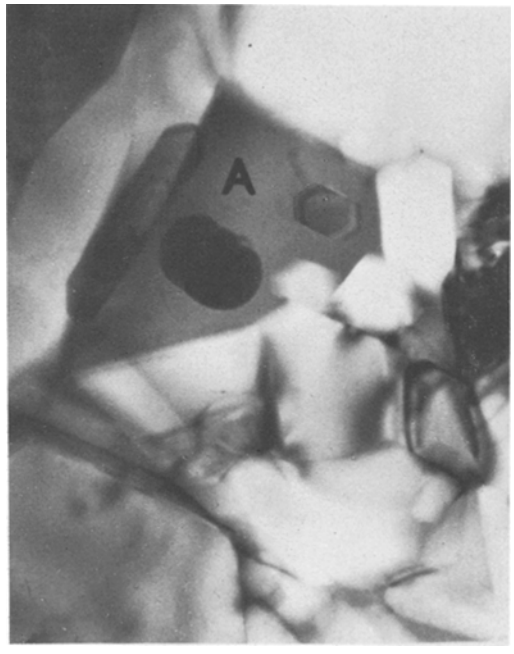

Figure 34 Transmission electron micrograph of hot-pressed silicon nitride with amorphous (liquid) region "A" from which has grown a well-defined hexagonal β-Si_3N_4 crystal, × 20 000.

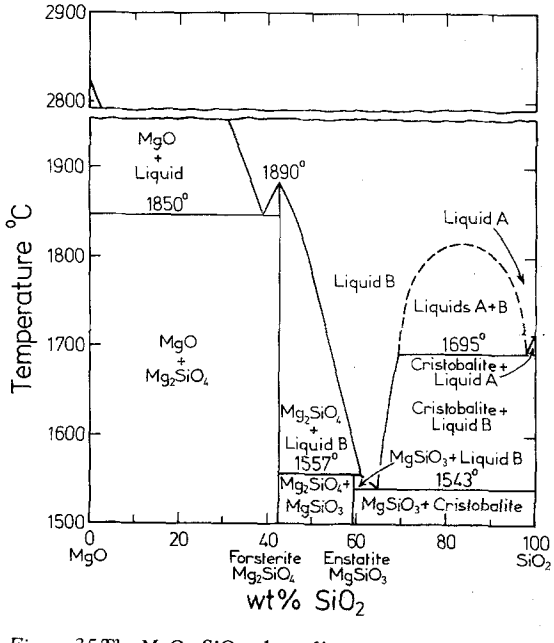

Figure 35 The MgO–SiO_2 phase diagram.

diffraction patterns of enstatite and cristobalite; with addition of 10 wt% Si_3N_4 no diffraction pattern at all is observed. Magnesium "silicate" glasses containing up to 10 at.% nitrogen have been prepared and on devitrification at 1500° C

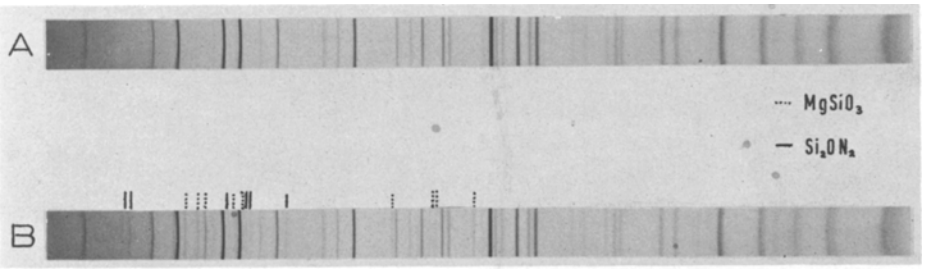

Figure 36 X-ray photographs showing the devitrification of the glassy phase in silicon nitride hot-pressed with 10 wt% MgO.

give mixtures containing enstatite, cristobalite, and silicon oxynitride.

Other nitrogen glasses occur in the lithium–sialon and yttrium–sialon systems. For example, by melting a mixture of molar composition $14Y_2O_3:59SiO_2:27AlN$ in a graphite crucible lined with boron nitride at 1650°C under nitrogen, and then air-cooling to room temperature, a completely vitreous product was obtained. Microscopic and X-ray examination showed it to be a glass, transparent in thin sections with a refractive index of about 1.76. Nitrogen analyses gave 9 at.%, only slightly less than the nitrogen content of the starting mix, and devitrification by heat-treatment for 16h at 1200°C or by slow cooling from 1650°C gave a crystalline product showing diffraction patterns of β-$Y_2O_3 \cdot 2SiO_3$, $3Y_2O_3 \cdot 5Al_2O_3$ (yttrium–aluminium garnet, YAG) and Si_2N_2O.

Even small concentrations of nitrogen not exceeding 1 at.% in oxide glasses are reported [39–41] to increase the softening temperature, viscosity, and the resistance to devitrification. Glasses with 10 at.% N or more might be expected to have more unusual properties. If in the tetrahedral network the nitrogen is co-ordinated by three ligands the structure should be more rigid and hence have a higher viscosity than the silicate glasses. The prospect of producing glasses more refractory and more resistant to devitrification than vitreous silica seems worth exploration.

The ease of shaping and the possibility of glass-ceramics in which the crystallising phases are refractory nitrides and oxynitrides suggest that nitrogen-containing glasses might eventually be just as important, from a technological viewpoint, as the crystalline sialons.

9. Conclusions

The acronym "sialon" was originally given to new compounds derived from silicon nitrides and oxynitrides by simultaneous replacement of silicon and nitrogen by aluminium and oxygen. The discovery was made concurrently and independently at Newcastle-upon-Tyne and in Japan. It was soon realized that other metal atoms could be incorporated, and the term has become a generic one applied to materials where the structural units are (Si, Al) $(O, N)_4$ or (Si, M)$(O, N)_4$ tetrahedra.

Silicon nitride has the atomic arrangement of a silicate structure, phenacite, and the sialons are essentially silicates in which oxygen is partly replaced by nitrogen. It is not yet known whether the field of the sialons is as large as that of the silicates, but it is certainly extensive. It includes vitreous materials as well as crystalline phases, and the mutual replacement of oxygen and nitrogen gives an additional degree of freedom which seems worth exploring in many different directions. So far, this exploration has been superficial and there have been mistakes in the interpretation of experimental observations both in England and Japan. Sufficient of the principles are known, however, to make possible the more detailed and careful investigations that are now required to establish reliable preparative methods and to characterize the products more precisely.

Scientifically, the new materials are of interest because their interatomic bonding is likely to cover a wide spectrum from partly ionic, as in the oxides, to highly covalent. The prospect of completely new types of crystal structure seems promising, and the correlation of properties with structure will be a rewarding but formidable task. It is of interest to speculate on the existence of even more varied tetrahedral structural units, for example containing boron and carbon, or even phosphorus and sulphur. There is little doubt that sialon-type oxynitrides exist in which germanium occurs instead of silicon, but these are unlikely to contribute much of scientific value.

Technologically, the discovery of sialons is important because of the current interest in engineering ceramics and the distinct possibility of improving properties and fabrication methods by the use of "ceramic alloys". Recent improvements in the strength, creep-resistance and oxidation-resistance of hot-pressed silicon nitride all involve an understanding of oxide–nitride interactions and the formation of oxynitride glasses; improved fracture toughness seems possible by the control of mixed sialon microstructures; and a final goal – pressureless sintering to theoretical density – can be achieved more easily with sialons than with silicon nitride.

The metallurgical applications of some of the sialons for holding and conveying molten metals are probably of more immediate importance than their use as engineering ceramics. Also, their abrasive properties have not been explored. Sialons are certainly not all going to be useful as ceramics but their potentialities in other directions should not be neglected. Preliminary measurements of the electrical conductivity of lithium sialons suggests that the current carriers are lithium ions and that there might be possibilities here for solid electrolytes. The AlN-polytypes with different M/X ratios are unusual variants of the wurtzite structure and so semi-conduction is not impossible. Aluminium is generally four-co-ordinated in the sialons and so the catalytic properties compared with those of alumina should be investigated, particularly in the synthesis of nitrogen-containing compounds. Finally, although manganese, copper and zinc can be accommodated as well as lithium, magnesium and yttrium in sialon structures, the limits of substitution have not been explored and no work at all has been carried out on the incorporation of elements of variable valency.

The preparation of sialon glasses containing – so far – as much as 10 at. % nitrogen opens up a further field. If nitrogen can replace oxygen in the crystalline silicates, perhaps it is not surprising that similar replacement occurs in the vitreous silicates.

It can be concluded that the sialons offer exciting and almost unlimited prospects for scientific investigation and technological development.

Acknowledgements

I thank all my colleagues in the Wolfson Research Group, and particularly Dr D.P. Thompson, for help in preparing this review of their work. Most of the research, except for that on lithium sialons supported by the Ministry of Defence, has been financed by Joseph Lucas Limited and the Wolfson Foundation.

References

1. N. L. PARR, G. F. MARTIN and E. R. W. MAY, "Study and Application of Silicon Nitride as a High Temperature Material", Admiralty Materials Laboratory Report No. A/75(s) (1959).
2. N. L. PARR, *Research (London)* **13** (1960) 261.
3. Report of the Committee on Motor Vehicle Emissions. 1973 Washington, D.C: National Academy of Sciences.
4. D. W. RICHERSON, *Amer. Ceram. Soc. Bull.* **52** (1973) 560.
5. K. H. JACK, Ceramics for High-Performance Applications. Proceedings of the Second Army Materials Technology Conference at Hyannis, November 1973; (Brook Hill, Chestnut Hill, Massachusetts, 1974) p. 265.
6. K. H. JACK, *Trans. J. Brit. Ceram. Soc.* **72** (1973) 376.
7. Y. OYAMA and O. KAMIGAITO, *Japan J. Appl. Phys.* **10** (1971) 1637.
8. Y. OYAMA, *ibid* **11** (1972) 760.
9. K. H. JACK and W. I. WILSON, *Nature Phys. Sci. (London)* **238** (1972) 28.
10. I. COLQUHOUN, S. WILD, P. GRIEVESON and K. H. JACK, *Proc. Brit. Ceram. Soc.* **22** (1973) 207.
11. WASHBURN, M. E. *Amer. Ceram. Soc. Bull.*, **46** (1967) 667.
12. S. WILD, P. GRIEVESON and K. H. JACK, "The Crystal Chemistry of Ceramic Phases in the Silicon-nitrogen-oxygen and Related Systems", 1968 Progress Report No. 1, Ministry of Defence Contract N/CP.61/9411/67/4B/MP 387. See "Special Ceramics, 5", edited by P. Popper, Brit. Ceram. R.A., Stoke-on-Trent, 1972) p. 289.
13. A. TSUGE, H. INOUE and K. KOMEYA, Tenth Symposium on Basic Ceramics, Osaka, (1972).
14. Y. OYAMA, *Yogyo-Kyokai-Shi* **82** (1974) 351.
15. R. J. LUMBY, B. NORTH and A. J. TAYLOR, "Special Ceramics 6" Brit. Ceram. R.A., Stoke-on-Trent, (1975) p. 283.
16. L. J. GAUCKLER, H. L. LUKAS and G. PETZOW, presented at the Second Powder Metallurgical Seminar at the Max-Planck-Institut, Stuttgart, (1974). See *J. Amer. Ceram. Soc.* 58 (1975) 346.
17. D. P. THOMPSON, P. ROEBUCK, A. W. J. M. RAE and K. H. JACK, presented at Journees d' Etude sur les Nitrures II, U.E.R. des Sciences, Limoges, 1975. Unpublished.
18. D. P. THOMPSON, *ibid*, unpublished.
19. J. ZERNIKE, "Chemical Phase Theory" (Kluwer, Deventer, Netherlands, 1955).
20. E. JÄNECKE, *Z. anorg. Chem.* **53** (1907) 319.
21. Y. OYAMA and O. KAMIGAITO, *Yogyo-Kyokai-Shi* **80** (1972) 327.

22. P. DREW and M. H. LEWIS, *J. Mater. Sci.* **9** (1974) 1833.
23. E. GUGEL, I. PETZENHAUSER and A. FICKEL, *Powder Met. Int.* **7** (1975) 66.
24. D. P. THOMPSON and K. H. JACK, to be published.
25. A. HENDRY, D. S. PERERA, D. P. THOMPSON and K. H. JACK, "Special Ceramics 6" (Brit. Ceram. R.A. Stoke-on-Trent, 1975) p. 321.
26. E. PARTHÉ, "Crystal Chemistry of Tetrahedral Structures" (Gordon & Breach, New York, 1964).
27. A.-M. LEJUS, *Rev. Hautes Temp. et Refract.* **1** (1964) 53.
28. K. KOMEYA, H. INOUE and A. TSUGE, *J. Amer. Ceram. Soc.* **57** (1974) 411.
29. S. UMEBAYASHI and K. KOBAYASHI, *Amer. Ceram. Soc.* **Bull 54** (1975) 534.
30. W. J. ARROL, Ceramics for High-Performance Applications. Proceedings of the Second Army Materials Technology Conference at Hyannis, November 1973 (Brook Hill, Chestnut Hill, Massachusetts, 1974) p. 729.
31. D. S. PERERA, D. P. THOMPSON and K. H. JACK, to be published.
32. G. E. GAZZA, *J. Amer. Ceram. Soc.* **56** (1973) 662.
33. A. W. J. M. RAE, D. P. THOMPSON, N. J. PIPKIN and K. H. JACK, "Special Ceramics 6" (Brit. Ceram. R.A., Stoke-on-Trent, 1975) p. 347.
34. A. W. J. M. RAE, D. P. THOMPSON and K. H. JACK, to be published.
35. A. TSUGE, H. KUDO and K. KOMEYA, *J. Amer. Ceram. Soc.* **57** (1974) 269.
36. P. L'HARIDON, M. MAUNAYE, Y. LAURENT and J. LANG, Presented at Journees d'Etude sur les Nitrures II, U.E.R. des Sciences, Limoges, 1975. See C. HAMON, R. MARCHAND, M. MAUNAYE, J. GAUDÉ and J. GUYADER, *Rev. Chimie minérale* **12** (1975) 259.
37. R. WILLS, *J. Amer. Ceram. Soc.* **57** (1974) 459.
38. K. NUTTALL and D. P. THOMPSON, *J. Mater. Sci.* **9** (1974) 850.
39. F. L. HARDING and R. J. RYDER, *Glass Tech.* **11** (1970) 54.
40. T. H. ELMER and M. E. NORDBERG, *J. Amer. Ceram. Soc.* **50** (1967) 275.
41. H. O. MULFINGER, *J. Amer. Ceram. Soc.* **43** (1966) 462.

Received 8 October and accepted 17 October 1975.